

A SURVEY FOR NEW MEMBERS OF THE TAURUS STAR-FORMING REGION WITH THE SLOAN DIGITAL SKY SURVEY¹

K. L. LUHMAN^{2,3}, E. E. MAMAJEK⁴, S. J. SHUKLA⁵, AND N. P. LOUTREL⁶

Draft version March 20, 2022

ABSTRACT

Previous studies have found that ~ 1 deg² fields surrounding the stellar aggregates in the Taurus star-forming region exhibit a surplus of solar-mass stars relative to denser clusters like IC 348 and the Orion Nebula Cluster. To test whether this difference reflects mass segregation in Taurus or a variation in the IMF, we have performed a survey for members of Taurus across a large field (~ 40 deg²) that was imaged by the Sloan Digital Sky Survey (SDSS). We obtained optical and near-infrared spectra of candidate members identified with those images and the Two Micron All Sky Survey, as well as miscellaneous candidates that were selected with several other diagnostics of membership. We have classified 22 of the candidates as new members of Taurus, which includes one of the coolest known members (M9.75). Our updated census of members within the SDSS field shows a surplus of solar-mass stars relative to clusters, although it is less pronounced than in the smaller fields towards the stellar aggregates that were surveyed for previously measured mass functions in Taurus. In addition to spectra of our new members, we include in our study near-IR spectra of roughly half of the known members of Taurus, which are used to refine their spectral types and extinctions. We also present an updated set of near-IR standard spectra for classifying young stars and brown dwarfs at M and L types.

Subject headings: planetary systems: protoplanetary disks — stars: formation — stars: low-mass, brown dwarfs — stars: luminosity function, mass function — stars: pre-main sequence

1. INTRODUCTION

The Taurus complex of dark clouds is one of the nearest star-forming regions ($d = 140$ pc, Wichmann et al. 1998; Loinard et al. 2005; Torres et al. 2007, 2009, 2012) and is relatively well-populated with ~ 400 known members. Many of its members reside in loose aggregates near the dark clouds while others are scattered more widely across the ~ 100 deg² extent of the cloud complex. Even in the aggregates, the stellar densities are only ~ 10 pc⁻³, which is 100–1000 times lower than the densities of the most compact clusters in other nearby star-forming regions. Because the stars and cloud cores in Taurus are so sparsely distributed, they have served as some of the best available targets for studying the formation of stars in relative isolation. The close proximity and low density of Taurus also made it amenable to observations with early telescopes at X-ray, infrared (IR), and radio wavelengths that had low sensitivity and resolution. As a result, much of the foundational observational work in the field of star formation has been performed in Taurus

(Kenyon et al. 2008).

Stars and brown dwarfs within Taurus have been sought with a variety of diagnostics of youth and membership, consisting of photometric variability (Joy 1945, 1949), emission lines (Feigelson & Kriss 1983; Herbig et al. 1986; Briceño et al. 1993, 1999), proper motions (Jones & Herbig 1979; Hartmann et al. 1991; Gomez et al. 1992), UV emission (Findeisen & Hillenbrand 2010; Gómez de Castro et al. 2015), optical and near-infrared (IR) photometry (Luhman & Rieke 1998; Briceño et al. 1998, 2002; Martín et al. 2001; Luhman et al. 2003a; Luhman 2000, 2004, 2006; Guieu et al. 2006; Slesnick et al. 2006), X-ray emission (Feigelson & Kriss 1981; Walter & Kuhl 1981; Feigelson et al. 1987; Walter et al. 1988; Strom & Strom 1994; Neuhäuser et al. 1995; Carkner et al. 1996; Wichmann et al. 1996; Briceño et al. 1997, 1999; Güdel et al. 2007; Scelsi et al. 2007, 2008), and mid-IR emission (Beichman et al. 1986, 1992; Harris et al. 1988; Myers et al. 1987; Kenyon et al. 1990, 1994; Rebull et al. 2010, 2011; Luhman et al. 2006, 2009a,b; Mooley et al. 2013; Esplin et al. 2014). Each survey has been capable of finding members that have specific ranges of mass, extinction, location, and evolutionary stage. The current census of members has the highest level of completeness in ~ 1 deg² fields surrounding the richest stellar aggregates. The initial mass function (IMF) constructed from the known members within those fields (Briceño et al. 2002; Luhman 2004; Luhman et al. 2009b) exhibits a large surplus of solar-mass stars relative to the mass functions of clusters like the Orion Nebula Cluster, IC 348, and Chamaeleon I (Hillenbrand 1997; Hillenbrand & Carpenter 2000; Muench et al.

¹Based on observations performed with the Sloan Digital Sky Survey, Hobby-Eberly Telescope, NASA Infrared Telescope Facility, Gemini Observatory, and Canada-France-Hawaii Telescope.

²Department of Astronomy and Astrophysics, The Pennsylvania State University, University Park, PA 16802; kluhman@astro.psu.edu

³Center for Exoplanets and Habitable Worlds, The Pennsylvania State University, University Park, PA 16802, USA

⁴Department of Physics and Astronomy, The University of Rochester, Rochester, NY 14627

⁵Institute of Astronomy, Madingley Road, Cambridge CB3 0HA, UK

⁶eXtreme Gravity Institute, Department of Physics, Montana State University, Bozeman, MT 59715

2002, 2003; Luhman et al. 2003b; Luhman 2007). Given that more massive stars are often found preferentially near the centers of star-forming clusters (e.g., Hillenbrand & Hartmann 1998; Muench et al. 2003), it is plausible that the anomalous nature of the IMF measured in the Taurus aggregates is at least partially due to mass segregation.

To better determine the degree to which the IMF in Taurus differs from mass functions in other nearby star-forming regions, we have performed a survey for new members of Taurus across a large area of the region ($\sim 40 \text{ deg}^2$) using optical images from the Sloan Digital Sky Survey (SDSS; York et al. 2000; Finkbeiner et al. 2004) in conjunction with near-IR data from the Two Micron All Sky Survey (2MASS, Skrutskie et al. 2006). In our presentation of this survey, we begin by compiling a list of all known members of Taurus from previous studies (Section 2). We then select candidate members based on their positions in color-magnitude diagrams constructed from SDSS and 2MASS data and several other diagnostics of membership (Section 3) and use optical and near-IR spectra to measure their spectral types and assess their membership (Section 4). We conclude by using our updated census of members to check for IMF variations between the SDSS fields, the smaller regions surrounding the stellar aggregates in Taurus, and denser clusters like IC 348 (Section 5).

2. CENSUS FROM PREVIOUS STUDIES

Before presenting our survey for new members of Taurus, we describe the list of previously known members that we have adopted. We began with the census compiled by Luhman et al. (2009b, 2010), which consisted of 352 members that are resolved by 2MASS or the Infrared Array Camera (IRAC; Fazio et al. 2004) on the *Spitzer Space Telescope* (Werner et al. 2004). The components of a given multiple system that are unresolved in those images appear as a single entry. We now reject two of the stars from that catalog, HBC 372 and HBC 407. HBC 372 has been previously described as a relatively old, Li-depleted member of Taurus (Sestito et al. 2008). However, it is sufficiently faint relative to other Taurus members near its spectral type ($\sim 3.4 \text{ mag}$ below the median sequence) that it is not plausibly related to the star-forming event that produced the known members. We note that an edge-on disk cannot explain the faint photometry for this star since it does not exhibit evidence of a disk in mid-IR photometry (Luhman et al. 2010; Esplin et al. 2014). HBC 407 is rejected because its proper motion (e.g., Bertout & Genova 2006; Ducourant et al. 2005; Roeser et al. 2010; Zacharias et al. 2013) differs from those of the known members (Luhman et al. 2009b).

To the list of members from Luhman et al. (2009b, 2010), we have added the 25 new members from Esplin et al. (2014), the three young stars with proper motions consistent with membership from Findeisen & Hillenbrand (2010), and four new members from Rebull et al. (2010), consisting of 2MASS J04251550+2829275, 2MASS J04355760+2253574, 2MASS J04355949+2238291, and 2MASS J04380191+2519266. Esplin et al. (2014) described evidence of membership from previous studies for HD 285957, V1195 Tau, HD 31305, HD 286178, and

RXJ 0432.7+1809, which are included in our census. We also adopt the following stars as members: LH 0419+15 based on Li absorption and gravity-sensitive spectral features (Reid & Hawley 1999, this work)⁷, 2MASS J04242321+2650084 based on IR excess emission and proper motion (Rebull et al. 2010; Cieza et al. 2012; Zacharias et al. 2013), RXJ 0432.8+1735 based on Li absorption, IR excess emission, and proper motion (Carkner et al. 1996; Martín & Magazzù 1999; Padgett et al. 2006), and SST Tau 041831.2+282617 based on mid-IR spectral features (Furlan et al. 2011). We arrive 391 known members of Taurus from previous studies that are resolved by 2MASS or IRAC. In this work, we have identified 22 additional members, resulting in a total of 413 known members. We present the full sample of members in Table 1.

In a multiplicity survey of Taurus members, Daemgen et al. (2015) included an “extended sample” of G-K stars that was described as co-moving with the traditional members and associated with the Taurus clouds, but was relatively old based on weak Li absorption ($\sim 20 \text{ Myr}$). We find that most of the stars in that extended sample have proper motions or radial velocities that are inconsistent with a physical association with the traditional members (e.g., Wichmann et al. 2000; Roeser et al. 2010; Zacharias et al. 2013). In addition, the Li strengths of most of those stars are consistent with ages of $\sim 100 \text{ Myr}$ based on a comparison to the Pleiades (Soderblom et al. 1993). It is possible that a few stars in the extended sample from Daemgen et al. (2015) are associated with Taurus, but none show convincing evidence of membership, and the sample is likely dominated by young main sequence stars that are unrelated to Taurus (Briceño et al. 1997).

3. IDENTIFICATION OF CANDIDATE MEMBERS

For the purposes of commissioning, testing, and calibration, SDSS obtained images of areas that were outside of the official survey region (Finkbeiner et al. 2004). Portions of the Taurus star-forming region were included in those extra observations. In Figure 1, the SDSS fields in Taurus are indicated in a map of the dark clouds and known members. Finkbeiner et al. (2004) reported imaging of the field outlined in blue, which covers $\sim 40 \text{ deg}^2$. The area marked in red was observed by SDSS after that study. We have searched for members of Taurus in the field from Finkbeiner et al. (2004), and have not utilized the newer SDSS data.

The SDSS observations described by Finkbeiner et al. (2004) were not included in the early data releases for SDSS, and instead were processed and disseminated separately in that study. All of the SDSS data in Taurus have been part of the official data releases starting with Data Release 8 (Aihara et al. 2011). The version of the photo pipeline in those later releases was v5_6_3, which was updated somewhat from version v5_4_25 used in Finkbeiner et al. (2004). The algorithmic changes between these reductions were small and the resulting photometric measurements were unchanged at the

⁷ Esplin et al. (2014) reported that LH 0419+15 exhibited excess emission at $12 \mu\text{m}$ from the *Wide-field Infrared Survey Explorer* (*WISE*, Wright et al. 2010), but the detection in that band appears to be spurious based on closer inspection of those images.

$\sim 2\%$ level. For our study, we used the original version of the data that was presented by Finkbeiner et al. (2004). In their catalog of sources detected by SDSS, Finkbeiner et al. (2004) reported photometry for a number of aperture sizes. We have used their magnitudes for an aperture radius of $1''.745$. The SDSS images were obtained in the u , g , r , i , and z filters. Because we are searching for stars that are cool and are reddened by dust extinction, the latter two bands offer the greatest sensitivity for our survey. For each SDSS source, we searched for a counterpart within $1''$ in the 2MASS Point Source Catalog, which provides photometry in J , H , and K_s . Approximately 2 million sources were detected in both SDSS and 2MASS in the field from Finkbeiner et al. (2004).

To identify candidate members of Taurus with SDSS and 2MASS, we constructed extinction-corrected diagrams of $i - z$, $i - K_s$, and $H - K_s$ versus H , which are shown in Figure 2. The extinctions for sources in these diagrams were estimated in the manner described by Luhman et al. (2003a). In each color-magnitude diagram (CMD), we have marked a boundary along the lower envelope of the sequence formed by most known members for use in selecting candidate members. We have omitted the field stars appearing below the boundaries so that the known members in those areas of the diagrams can be more easily seen. Several known members are unusually faint for their colors and fall below the boundaries in the CMDs, which is normally attributed to scattered light dominating the observed flux. Some of those members are known to have edge-on disks or protostellar envelopes, and most of the others have been suspected of harboring such structures based on similar CMDs from previous studies. We identified sources as candidate members if they appeared above the boundaries in both the $i - K_s$ and $H - K_s$ CMDs, were not rejected in the $i - z$ CMD, were not rejected as non-members based on proper motions (Roeser et al. 2010; Zacharias et al. 2013), and exhibited $J - H > 0.5$ ($\gtrsim K4$) after correction for extinction. We describe spectroscopy of the resulting candidates in the next section.

In addition to the candidates from the CMDs in the SDSS field, we have selected for spectroscopy a sample of miscellaneous candidates that were identified with several other methods. One of these candidates, 2MASS J04144158+2809583, was selected based on its colors in images from IRAC on *Spitzer* and WIRCam on the Canada-France-Hawaii Telescope (CFHT). The WIRCam images were taken in the J , H , and K_s filters and cover 0.8 deg^2 of the B209 cloud, which contains the westernmost rich aggregate in Taurus. They were obtained through program 05BF35 (J.-L. Monin) and are publicly available in the CFHT archive. We measured photometry for all sources detected in those images and matched them to objects detected by IRAC (Luhman et al. 2006, 2010). To search for low-mass brown dwarfs ($>M8$) in those data, we applied the following criteria: not detected in optical images from the Digitized Sky Survey, not resolved as a galaxy in the WIRCam images, not previously classified as a member or non-member, $H < 17$, $H - K_s > 0.6$, $K_s - [4.5] > 0.7$ where $[4.5]$ is the $4.5 \mu\text{m}$ band of IRAC, $H - K_s > J - H - 0.7/1.55 + 0.4$, and photometric errors less than 0.1 mag in J , H , K_s , and $[4.5]$. These criteria produced

one candidate, 2MASS J04144158+2809583. We also selected for spectroscopy several objects from the IRAC surveys of Taurus that are candidate disk-bearing stars based on their red mid-IR colors (Luhman et al. 2006, 2010) and three stars from previous studies that have evidence of membership from proper motions (Roeser et al. 2010; Zacharias et al. 2013) and signatures of youth in the form of $H\alpha$ emission (Kohoutek et al. 1999), X-ray emission, or red mid-IR colors from *WISE*. Finally, we obtained spectra of a candidate companion to IRAS 04125+2902 identified by Luhman et al. (2009b) and a candidate companion to GZ Aur that was noticed during our spectroscopy of that star.

4. SPECTROSCOPY

4.1. Observations

We have obtained optical and near-IR spectra of 40 candidate members of Taurus that were selected in the previous section and possible companions to two of these candidates. We also observed 104 known members to improve the measurements of their spectral types and extinctions. The spectra were collected with the Gemini Near-Infrared Imager (NIRI, Hodapp et al. 2003) using the K -band grism and $0''.47$ slit ($1.9\text{--}2.5 \mu\text{m}$, $R = 700$), the Gemini Multi-Object Spectrograph (GMOS, Hook et al. 2004) using the 400 l mm^{-1} grating and $0''.75$ slit ($0.56\text{--}1 \mu\text{m}$, $R = 1500$), the Marcario Low-Resolution Spectrograph (LRS) on the Hobby-Eberly Telescope (HET) using the G3 grism and $2''$ slit ($0.63\text{--}0.91 \mu\text{m}$, $R = 1100$), and SpeX (Rayner et al. 2003) at the NASA Infrared Telescope Facility (IRTF) using either the prism or SXD mode ($R = 150/750$) and $0''.8$ slit ($0.8\text{--}2.5 \mu\text{m}$). The SpeX data were reduced with the Spextool package (Cushing et al. 2004) and corrected for telluric absorption in the manner described by Vacca et al. (2003). The spectra from the other instruments were reduced with similar methods using routines within IRAF.

In the next section, we classify 22 and 18 of the candidates in our spectroscopic sample as members and non-members, respectively. Two of these members have candidate companions that were also observed spectroscopically, both of which have uncertain membership based on our spectra. The members and non-members are listed in Tables 2 and 3, respectively, which provide the spectral classifications, the methods of selection, and the instruments and dates for the spectroscopy. The dates of the SpeX observations are also indicated for both new and previously known members in Table 1.

The optical spectra are presented in Figure 3, which apply to one previously known member (FT Tau) and five new members. The near-IR data for members are shown in Figures 4–11, which consist of 19 spectra of new members and 180 spectra in 178 previously known systems (both components of two binaries were observed). We have also included the spectra of the two candidate companions to new members that have uncertain membership (see Table 1). Four and 197 of those spectra were taken with NIRI and SpeX, respectively. The NIRI spectra are shown after smoothing to the resolution of the SpeX data. We have included all SpeX data for Taurus members from our previous studies (Luhman 2006; Luhman et al. 2006, 2007, 2009a,b; Muench et al. 2007;

Esplin et al. 2014), which correspond to 76 spectra in 75 systems.

4.2. Spectral Classification

We have measured spectral types for the candidate members and previously known members of Taurus in our spectroscopic sample and have assessed the membership of the former. We have also estimated extinctions for the members using the SpeX data, which are sensitive to extinction because they span a large range of wavelengths (0.8–2.5 μm).

The candidates can be divided into the following categories based on their spectra and other properties: highly redshifted emission lines (galaxies); absorption lines from hydrogen and metals (early-type stars and giants behind Taurus); red, featureless spectra and mid-IR excess emission (protostars in Taurus); absorption bands from TiO, VO, and H₂O (M-type objects in the field and in Taurus). To distinguish between field dwarfs and Taurus members in the latter category, we used gravity sensitive absorption features (Na I, K I, H₂O) and, when available, signatures of youth in the form of strong emission lines and mid-IR excess emission. As done in our previous studies (Luhman 1999), we measured spectral types from the optical spectra of the young objects through comparison to field dwarfs and averages of dwarfs and giants for $<M5$ and $\geq M5$, respectively (Henry et al. 1994; Kirkpatrick et al. 1991, 1997). The near-IR spectra were classified with standard spectra from our previous work, Cushing et al. (2005), and Rayner et al. (2009) for the field dwarfs and with standard spectra from the Appendix for the young objects. The errors for the optical and IR types are ± 0.25 and 0.5 subclass, respectively, unless indicated otherwise. The spectral types for the new members and non-members are listed in Tables 2 and 3, respectively. The former are also included in the compilation of classifications for all known members in Table 1. For previously known members that have SpeX classifications that are more uncertain than those available from previous optical spectroscopy, or that serve as near-IR classification standards (Appendix), we do not report a spectral type from SpeX, and instead adopt the previous optical type.

For Taurus members that have measured spectral types and that were observed with SpeX, we have estimated extinctions by comparing the observed spectral slopes at 1 μm to the slopes of our young standards. If the spectral type from SpeX was uncertain and a more accurate type was available from optical data in a previous study, then we adopted that classification when estimating the extinction. If the signal-to-noise (S/N) at 1 μm was low, then we estimated the extinction from the slope at longer wavelengths if an absence of mid-IR excess emission indicated that *K*-band excess was unlikely to be present. The resulting extinctions were used for dereddening the spectra in Figures 5–11. For Taurus members that have measured spectral types but were not observed by SpeX, we have estimated extinctions with the methods described by Furlan et al. (2011), such as $J - H$ and $J - K$. Our extinction estimates are presented in Table 1. For some of the objects for which we used the same methods as Furlan et al. (2011), our estimates differ from their values because of differences in the adopted spectral types. Our measurements of A_J from the SpeX

data have uncertainties of ~ 0.1 mag for objects that lack strong near-IR excess emission from disks and that have low-to-moderate extinctions ($A_J \lesssim 2$). The uncertainties are larger for the remaining members, particularly when strong excess emission is present throughout the near-IR bands. Most of the SpeX extinctions agree with the values from the alternative methods in Furlan et al. (2011) to within $A_J < 0.3$ and 0.1 mag for objects with and without large near-IR excesses, respectively.

4.3. Comments on Individual Sources

2MASS J04345973+2807017. Luhman et al. (2009b) identified it as a candidate based on mid-IR excess emission. They obtained a SpeX spectrum that was consistent with either a field dwarf or a young star, but it appeared to agree better with the former. However, the gravity sensitive features in our optical spectrum do indicate that it is young. As noted in Luhman et al. (2009b), it is much fainter than other members near its spectral type, which indicates that it is either a background young star that is not associated with Taurus or a member that is seen in scattered light. We assume the latter for the purposes of this work.

2MASS J04153452+2913469. It was selected for spectroscopy based on its mid-IR excess in photometry from *WISE* (Rebull et al. 2011; Esplin et al. 2014). Rebull et al. (2011) referred to it as a known galaxy, possibly because it is labeled as such by SDSS. Our NIRI acquisition image obtained prior to spectroscopy resolved it as a pair of sources that are separated by $0''.6$, as shown in Figure 12. It is unclear which component dominates the mid-IR flux detected by *WISE*. The spectrum of the northern component contains Br γ emission and CO absorption, which are indicative of a young low-mass star (Figure 4). The southern component exhibits extended emission that could be consistent with either a galaxy or reflection nebulosity surrounding a young star. If it is the latter, then it is probably a protostar based on its red, featureless spectrum.

5. INITIAL MASS FUNCTION

5.1. Completeness in the SDSS Field

We have attempted to perform a thorough survey for new members of Taurus within the SDSS field from Finkbeiner et al. (2004) in an effort to measure the IMF across a large portion of this region. To construct an IMF from our updated census of Taurus members within the SDSS field, we have begun by characterizing the completeness of that census. As in our previous IMF studies of this kind, we have investigated the completeness using a near-IR CMD because it is sensitive to members at low masses and high extinctions. In Figure 13, we show a diagram of K_s versus $H - K_s$ based on 2MASS data for the known members of Taurus and other sources with unconstrained membership within the SDSS field. We have omitted objects that are likely to be non-members based on the CMDs in Figure 2, proper motions, or spectroscopy from this work and previous studies. The CMD in Figure 13 indicates that the census of Taurus members within the SDSS field from Finkbeiner et al. (2004) has a high degree of completeness for large ranges of magnitude and extinction. Therefore, a sample of known members in the SDSS field that have extinctions below

a given threshold should be representative of the IMF in that field down to a certain mass, assuming that the average extinction does not vary with mass. For our IMF sample, we have selected a threshold that is high enough to encompass a large number of members while low enough that the sample has a high level of completeness down substellar masses, arriving at $A_J < 3$. Based on Figure 13, the current census in the SDSS field is nearly complete for extinction-corrected magnitudes of $K_s < 12.7$ within that threshold, which corresponds to masses of $\lesssim 0.03 M_\odot$ for ages of a few Myr according to evolutionary models (Baraffe et al. 1998, 2015).

5.2. Comparison to XEST Fields and IC 348

The completeness limit of $0.03 M_\odot$ for our extinction-limited sample in the SDSS field is similar to the limit of $0.02 M_\odot$ for the IMF in the XEST fields from Luhman et al. (2009b). As a result, the two mass functions can be directly compared. In particular, we would like to check whether the surplus of solar-mass stars in the XEST fields relative to other star-forming regions is also present across a larger area like the SDSS field (see Section 1).

Masses of young stars are typically derived by combining estimates of bolometric luminosities (from photometry) and effective temperatures (from spectral types) with the values predicted by evolutionary models. However, because these mass estimates are subject to uncertainties in the adopted bolometric corrections, temperature scales, and models, and because we are primarily interested in detecting variations in the IMF between different samples of young stars, we have chosen to use the distributions of spectral types in those samples as observational proxies for their IMFs. The ages of Taurus and IC 348 derived from comparisons of their low-mass stars to theoretical isochrones are sufficiently similar (~ 1 and 2 Myr, Luhman et al. 2003b) that a given spectral type should correspond to the same mass in both regions. It has been suggested that isochronal ages for star-forming regions may be underestimated by a factor of ~ 2 (Naylor 2009; Bell et al. 2013). Even if that is true for one of the two regions, the relationships between spectral types and masses should still be nearly identical between the regions for masses of $\lesssim 1.5 M_\odot$ according to evolutionary models (Baraffe et al. 1998).

In Figure 14, we show the spectral type distributions for our extinction-limited sample in the SDSS field. For comparison, we also include the IMF sample in the XEST fields (Luhman et al. 2009b) and an extinction-limited sample in IC 348 (Luhman et al. 2016), which is representative of IMFs in nearby star-forming clusters (Hillenbrand 1997; Luhman 2007). The sample of members in the SDSS field exhibits a surplus of stars near M0 ($\sim 0.7 M_\odot$) relative to IC 348, but it is smaller than that in the XEST fields. This indicates that the solar-mass stars are slightly concentrated near the aggregates, and that the IMF on large scales in Taurus does differ from denser clusters. Thus, it appears that previously reported differences in IMFs between Taurus and denser clusters were a reflection of modest levels of both mass segregation and IMF variations.

5.3. Effects of Magnetic Activity

We now discuss a recently proposed source of systematic error in measurements of IMFs in Taurus and other star-forming regions. The young eclipsing binary brown dwarf 2MASS J05352184–0546085 exhibits an anomaly in which the primary is cooler than the secondary (Stassun et al. 2006), which has been attributed to a reduction of the primary’s temperature by magnetic activity (Reiners et al. 2007; Stassun et al. 2007). If the spectral types of young stars and brown dwarfs can be significantly affected by activity, then their mass estimates, and hence their IMFs, may contain large systematic errors (Mohanty et al. 2009). Stassun et al. (2012, 2014) attempted to quantify those errors, concluding that the masses derived from spectral types could be underestimated by up to a factor of two. Such error estimates depend on the adopted conversion between spectral types and temperatures; a temperature scale for inactive stars was used in those studies. However, if one instead derives masses with a scale for active stars, the systematic errors would be much smaller. For instance, the widely adopted scale from Luhman et al. (2003b) was designed for use with young stars and brown dwarfs, and thus may account for the typical effects of activity in such populations. Systematic errors can arise at multiple stages in the derivation of masses for young stars (e.g., temperature scale, evolutionary models), regardless of whether activity is responsible for some of those errors. The most important question is whether the combination of those various stages produce masses that are accurate (Luhman 2012). As discussed by Luhman & Potter (2006) and Luhman (2012), the IMFs of low-mass stars and brown dwarfs that we have previously derived for star-forming clusters are consistent with mass functions of open clusters (Morau et al. 2004) and the solar neighborhood (Reid et al. 2002; Bochanski et al. 2010; Kirkpatrick et al. 2012), and thus show no evidence of large systematic errors.

6. CONCLUSIONS

We have attempted to measure the IMF across a larger fraction of Taurus than considered in previous IMF studies of this region to better determine whether it exhibits an anomalous IMF relative to denser nearby clusters like IC 348. To do this, we have performed a thorough survey for new members within a ~ 40 deg² field that was imaged by SDSS. We have obtained spectra of candidate members appearing in CMDs for that field, as well as a miscellaneous sample of candidates across all of Taurus that were selected with a variety of diagnostics of membership. Through our spectroscopy, we have classified 22 candidates as new members, which includes one of the coolest known members (M9.75). The update census of Taurus now contains 413 members that are resolved by 2MASS or *Spitzer*. For the SDSS field, we have constructed an extinction-limited sample of members that should be nearly complete down to masses of $\sim 0.03 M_\odot$. That sample exhibits a surplus of solar-mass stars relative to clusters like IC 348, although it is less pronounced than in previously reported IMFs in Taurus that have been measured for smaller fields. *Gaia* (Perryman et al. 2001) and Pan-STARRS1 (Kaiser et al. 2002) will soon provide photometry and astrometry that can be used to search the entire extent of the Taurus cloud complex for new members down to substellar masses and at low-to-

moderate extinctions, which will further improve the statistical accuracy of the measurement of the IMF.

K. L. acknowledges support from NSF grant AST-1208239 and E. M. acknowledges support from NSF grant AST-1313029 and the NASA NExSS program. We thank Jackie Faherty for providing her SpeX data and David Schlegel and Doug Finkbeiner for information regarding the SDSS data. The Gemini data were obtained through program GN-2009B-Q-91. Gemini Observatory is operated by AURA under a cooperative agreement with the NSF on behalf of the Gemini partnership: the NSF (United States), the NRC (Canada), CONICYT (Chile), the ARC (Australia), Ministério da Ciência, Tecnologia e Inovação (Brazil) and Ministerio de Ciencia, Tecnología e Innovación Productiva (Argentina). The IRTF is operated by the University of Hawaii under contract NNH14CK55B with NASA. 2MASS is a joint project of the University of Massachusetts and IPAC at Caltech, funded by NASA and the NSF. Funding for SDSS has been provided by the Alfred P. Sloan Foundation, the Participating Institutions, the NSF, the U.S. Department of Energy, NASA, the Japanese Monbukagakusho, the Max Planck Society, and the Higher Education Funding Council for England. The SDSS Web Site is <http://www.sdss.org/>. The SDSS is managed by the Astrophysical Research Consortium for the Participating Institutions. The Participating Institutions are the American Museum of Natural History, Astrophysical Institute Potsdam, University of Basel, University of Cambridge, Case Western Reserve University, The University of Chicago, Drexel University, Fermilab, the Institute for Advanced Study, the Japan Participation Group, The Johns Hopkins University, the Joint Institute for

Nuclear Astrophysics, the Kavli Institute for Particle Astrophysics and Cosmology, the Korean Scientist Group, the Chinese Academy of Sciences, Los Alamos National Laboratory, the Max-Planck-Institute for Astronomy, the Max-Planck-Institute for Astrophysics, New Mexico State University, Ohio State University, University of Pittsburgh, University of Portsmouth, Princeton University, the United States Naval Observatory, and the University of Washington. The HET is a joint project of the University of Texas at Austin, the Pennsylvania State University, Stanford University, Ludwig-Maximilians-Universität München, and Georg-August-Universität Göttingen. The HET is named in honor of its principal benefactors, William P. Hobby and Robert E. Eberly. The Marcario Low-Resolution Spectrograph at HET is named for Mike Marcario of High Lonesome Optics, who fabricated several optics for the instrument but died before its completion; it is a joint project of the HET partnership and the Instituto de Astronomía de la Universidad Nacional Autónoma de México. WIRCam is a joint project of CFHT, Taiwan, Korea, Canada, and France. CFHT is operated by the NRC of Canada, the Institute National des Sciences de l'Univers of the Centre National de la Recherche Scientifique of France, and the University of Hawaii. This work used data from the SpeX Prism Spectral Libraries (maintained by Adam Burgasser at <http://www.browndwarfs.org/spexprism>), the NASA/IPAC Infrared Science Archive (operated by JPL under contract with NASA), and SIMBAD database, operated at CDS, Strasbourg, France. The Center for Exoplanets and Habitable Worlds is supported by the Pennsylvania State University, the Eberly College of Science, and the Pennsylvania Space Grant Consortium.

APPENDIX

NEAR-IR SPECTRAL STANDARDS FOR M AND L TYPES AT YOUNG AGES

Selection Criteria

If field dwarfs are used as the standards when measuring spectral types of young late-type objects at near-IR wavelengths, the resulting types are often systematically later than those that would be derived with optical spectroscopy because the depths of the strongest near-IR features, the steam bands, depend on surface gravity (Luhman et al. 2003b; Luhman 2012). In our previous studies, to measure IR spectral types that are tied to those at optical wavelengths, we have classified the IR spectra of young M-type stars via comparison to other young objects for which we have measured optical types. The number of young stars with both optical spectral types and IR spectra is now large enough that we can combine the spectra of several objects at each subclass for use as classification standards. To do this for ages of $\lesssim 10$ Myr, we consider objects that satisfy the following criteria: classified at optical wavelengths with our methods for M types or with those from Cruz et al. (2007, 2009, 2016) and Kirkpatrick et al. (2010) for L types; member of a nearby cluster or association that has an age of $\lesssim 10$ Myr or a member of the solar neighborhood that has an age of $\lesssim 100$ Myr based on gravity-sensitive spectral features; unlikely to have *K*-band excess emission from circumstellar dust based on near- to mid-IR photometry; and SpeX spectra that have $S/N \gtrsim 30$ and good telluric correction are available. Because of their uncertain ages, objects in the solar neighborhood are used only for spectral types in which there are few members of clusters that have accurate optical spectral types and adequate spectra, which corresponds to the L types. The surface gravities indicated by optical spectra have been previously denoted by suffixes of α (highest gravity), β , γ , and δ (lowest gravity) that are appended to spectral types (Kirkpatrick 2005; Kirkpatrick et al. 2006; Cruz et al. 2009). We have considered L dwarfs classified as γ or δ , which likely correspond to ages of ~ 10 – 100 and $\lesssim 10$ Myr, respectively.

New Data in TWA

Members of the TW Hya association (TWA) are especially appealing as spectral standards since they are nearby and are just old enough to no longer be obscured by their natal molecular cloud (30–80 pc, ~ 10 Myr, Webb et al. 1999; Mamaĵek 2005). We have observed many of those objects with optical spectroscopy to obtain optical spectral types that have been measured with our methods, facilitating their inclusion in our new standards. These data were

taken with the Goodman High Throughput Spectrograph at the Southern Astrophysical Research (SOAR) Telescope on the nights of 2014 May 8 and 9 (TWA 1, 2, 3A, 3B, 4, 5A, 6, 7, 8A, 8B, 10, 11C, 12, 13, 16, 20, 23, 25, 30, 32) and the Cerro Tololo Ohio State Multi-Object Spectrograph (COSMOS) at the 4 m Blanco telescope at Cerro Tololo Inter-American Observatory on the night of 2015 May 12 (TWA 26, 33, 34). Goodman was operated with the 400 l/mm grating in second order, the GG495 filter, and the 0".46 slit (3 Å resolution). COSMOS was configured with the red VPH grism, the OG530 filter, and slit widths of 0".9 (TWA 33 and 34, 3 Å) and 1".2 (TWA 26, 4 Å). The wavelength coverage was roughly 5500–9500 Å for both instruments. In Table 4, we have compiled previous spectral types and our new measurements for the known members of TWA. For TWA 29, we have included the spectral type that we have measured from the optical spectrum collected by Looper et al. (2007), which is nearly the same as one reported in that study. To provide the near-IR spectra needed for our standards, we also observed some of the members of TWA with the prism mode of SpeX (0".8 slit) on the nights of 2005 December 14 (TWA 1, 2, 5, 6, 7, 8A, 8B, 26, 27, 28), 2011 December 3 (TWA 13), and 2015 April 19–22 (TWA 10, 12, 11C, 23, 32, 33, 34).

Construction of Standard Spectra

After compiling SpeX data from this work and previous studies for objects that satisfied our selection criteria, we adjusted the slope of each spectrum among the M types using the reddening law of Cardelli et al. (1989) so that its $J - H$ color agreed with the typical intrinsic value for a young star at its optical spectral type (Luhman et al. 2010). This was done to correct for reddening by interstellar dust and to facilitate comparison of all spectra near a given spectral type. The spectral slopes of the L dwarfs were not dereddened since they reside in the solar neighborhood, and thus should have little extinction, and since the intrinsic colors of L dwarfs are not well-determined for the age range in which we are attempting to create spectral standards ($\lesssim 10$ Myr). We then compared the spectra of objects with similar optical types and rejected spectra that were outliers in the strengths of their absorption features relative to most other data. The unrejected spectra within bins of 0.5–1 subclass were combined with the appropriate weights based on their optical spectral types to produce a spectrum at each 0.5 subclass interval between M0–L0 and at L2, L4, and L7. We compared the spectra between younger and older populations (Taurus and IC 348 versus TWA and Upper Sco) and found that the 0.7–1.1 slopes were systematically redder at older ages for types of M3.5–M6.5. As a result, the spectra of the two populations were split into two standard spectra at each spectral type within that range. In Table 5, we list the objects used to create the standard spectra, the optical spectral types that were adopted for them, and dates of their SpeX observations. We show a sample of the standard spectra in Figure 15. The displayed spectra for M4 and M6 apply to the younger populations. Electronic versions of all of the standard spectra are available via Figure 15. The differences in the 0.7–1.1 slopes between the younger and older objects are illustrated in Figure 16, where we compare the standard spectra for the two populations at M4, M5, and M6.

Because the young L dwarfs that we considered exhibit large variations in their spectral slopes and poorly populate some subclasses, we describe for the individual L subclasses the spectra that we chose to use as standards and those that we rejected. In this discussion, we quantify differences in the slopes in the SpeX data between pairs of objects in terms of the amount of extinction, A_V , that would produce the same difference via reddening. At L0, 2MASS J01415823–4633574, 2MASS J22134491–2136079, 2MASS J23153135+0617146 have similar features and slopes in their SpeX data while 2MASS J02411151–0326587 is bluer by $A_V = 0.5$ and 2MASS J03231002–4631237 is redder by $A_V = 0.7$. Because of the agreement of the first three spectra, we adopted their mean spectrum as the standard for L0. For the one known member of Taurus with an optical spectral type of L0, 2MASS J04373705+2331080 (Luhman et al. 2009b), the SpeX spectrum from Bowler et al. (2014) agrees with our L0 standard except that the Taurus object is redder by $A_V = 2$, which is likely due to some combination of extinction and an intrinsically redder color. The latter is plausible given that it is likely younger than the field L dwarfs we have considered, and L dwarfs tend to have redder near-IR colors at younger ages (Kirkpatrick et al. 2006; Cruz et al. 2009). At L1, only 2MASS J05184616–2756457 satisfied our criteria for consideration as a standard, and its spectrum differs only slightly from the L0 standard in the depths of its steam bands and its spectral slope. Therefore, we have not adopted a standard spectrum for that spectral type. At L2, 2MASS 05361998-1920396 and 2MASS 00550564+0134365 have similar spectra except for a modest difference in their spectral slopes ($A_V = 0.4$), so we have adopted the mean of their spectra as the L2 standard. Among the L4 dwarfs that we examined, 2MASS J15382417–1953116 has the bluest spectrum, and 2MASS J05012406–0010452, 2MASS J15515237+0941148, 2MASS J01262109+1428057, and 2MASS J16154255+4953211 are redder by $A_V = 0.4, 0.4, 1.8,$ and 3 , respectively. The steam bands are slightly weaker in the latter two objects than in the others. We have adopted the mean of 2MASS J05012406–0010452 and 2MASS J01262109+1428057 as the L4 standard. The one L3 γ dwarf with a SpeX spectrum, 2MASS J22081363+2921215, is bluer than our adopted L2 standard, and thus does not follow the trend of redder spectra with later L types, making it unsuitable as a standard. The only two L5 dwarfs that we examined are 2MASS J05120636–2949540 and 2MASS J03552337+1133437; the former is similar to the L4 dwarfs and the latter is an outlier in its slope and the depths of its steam bands, so we have not adopted a standard at L5. Since optical spectral types have not been defined for young L dwarfs later than L5 (Cruz et al. 2009), we have adopted the near-IR types of L7 that have been proposed for TWA 41 and 42 (Kellogg et al. 2015; Schneider et al. 2016) and we take the mean of their spectra as the standard at that type. We note that the near-IR spectrum of the young late-L dwarf PSO J318.5338–22.8603 (Liu et al. 2013) is similar to the data for those TWA members except that it is redder by $A_V = 1.5$.

Application of the Standard Spectra

Our standard spectra have been designed for classifying M- and L-type objects that have ages of $\lesssim 10$ Myr. Most objects at these ages reside in clusters and associations that are embedded within molecular clouds. Populations like Upper Sco that are no longer associated with molecular clouds also can exhibit noticeable reddening ($A_V > 0.2$) from the interstellar medium beyond the Local Bubble ($d \gtrsim 100$ pc). As a result, to classify an object's spectrum with our standard spectrum, one should identify the combination of spectral type and reddening that provides the best fit. Even in the presence of reddening, it is normally possible to measure IR types with errors of only ± 0.5 at M types. However, because the depths of the steam bands do not vary significantly among the L types, there is greater degeneracy between spectral type and reddening, resulting in larger uncertainties in the two parameters. The degeneracy is illustrated in Figure 17, which shows that the unreddened standards at L2, L4, and L7 are similar to reddened versions of the standards at L0, L2, and L4, respectively. Because young L dwarfs at a given optical spectral type exhibit a fairly large range of spectral slopes (Section A.3), a similar degeneracy is present in the IR classifications of young L dwarfs in the solar neighborhood.

We have applied our standard spectra to a sampling of IR spectra that have been classified in other studies. We frequently arrive at types that are earlier than the previous results. Examples of three such objects are shown in Figure 18, where we compare their spectra to our best-fitting standards and our standards for the previously reported types. The first object, TWA 40, was previously classified as L0 and L1 at optical and IR wavelengths, respectively (Gagné et al. 2014, 2015). We find that our M9.5 standard provides the best match to its IR spectrum. The IR type from Gagné et al. (2015) was partially based on a comparison to members of Upper Sco that had been classified as L0–L1 with IR data (Lodieu et al. 2008). However, optical spectroscopy indicates that several of those sources in Upper Sco have spectral types near M9 (Herczeg et al. 2009, K. Luhman, in preparation), which would explain why Gagné et al. (2015) found a type later than our value. The second object in Figure 18, 2MASS J15575011–2952431, is a similar example of a source previously classified as early L (Allers & Liu 2013; Faherty et al. 2016) for which we measure a type near M9. Our IR classification agrees with the optical spectral type of that object (Kirkpatrick et al. 2010). Finally, we compare in Figure 18 the IR spectrum of 1RXS J160929.1–210524 B (Lafrenière et al. 2008, 2010) to our best-fitting standard (M9.5 with $A_V = 1.2$) and our standard for the type of L4 that was measured by Lafrenière et al. (2008) and Lachapelle et al. (2015). The companion agrees well with M9.5, and is too blue to be a typical young L4 dwarf. The extinction estimate from our classification is lower than the value of $A_V = 4.5$ derived by Wu et al. (2015) through a comparison of the observed near-IR spectral energy distribution to model predictions.

REFERENCES

- Aihara, H., Allende Prieto, C., An, D., et al. 2011, *ApJS*, 193, 29
- Allers, K. N., & Liu, M. C. 2013, *ApJ*, 772, 79
- Baraffe, I., Chabrier, G., Allard, F., & Hauschildt, P. H. 1998, *A&A*, 337, 403
- Baraffe, I., Horneimer, D., Allard, F., & Chabrier, G. 2015, *A&A*, 577, 42
- Beck, T. L. 2007, *AJ*, 133, 1673
- Beichman, C. A., Boulanger, F., & Moshir, M. 1992, *ApJ*, 386, 248
- Beichman, C. A., Myers, P. C., Emerson, J. P., et al. 1986, *ApJ*, 307, 337
- Bell, C. P. M., Naylor, T., Mayne, N. J., Jeffries, R. D., & Littlefair, S. P. 2013, *MNRAS*, 434, 806
- Bertout, C., & Genova, F. 2006, *A&A*, 460, 499
- Bochanski, J. J., Hawley, S. L., Covey, K. R., et al. 2010, *AJ*, 139, 2679
- Bonnefoy, M., Chauvin, G., Lagrange, A.-M., et al. 2014, *A&A*, 562, A127
- Boss, B. 1937, General Catalogue of 33342 stars for the epoch 1950. Vol.1: Introduction and explanatory tables; Right Ascension 6 h-12 h; Right Ascension 12 h-18 h; Vol. 5: Right Ascension 18 h-24 h
- Bowler, B. P., & Hillenbrand, L. A. 2015, *ApJ*, 811, L30
- Bowler, B. P., Liu, M. C., Kraus, A. L., & Mann, A. W. 2014, *ApJ*, 784, 65
- Briceño, C., Calvet, N., Gomez, M., et al. 1993, *PASP*, 105, 686
- Briceño, C., Calvet, N., Kenyon, S., & Hartmann, L. 1999, *AJ*, 118, 1354
- Briceño, C., Hartmann, L., Stauffer, J., & Martín, E. L., 1998, *AJ*, 115, 2074
- Briceño, C., Hartmann, L., Stauffer, J., et al. 1997, *AJ*, 113, 740
- Briceño, C., Luhman, K. L., Hartmann, L., Stauffer, J. R., & Kirkpatrick, J. D. 2002, *ApJ*, 580, 317
- Calvet, N., Muzerolle, J., Briceño, C., et al. 2004, *AJ*, 128, 1294
- Cardelli, J. A., Clayton, G. C., & Mathis, J. S. 1989, *ApJ*, 345, 245
- Carkner, L., Feigelson, E. D., Koyama, K., Montmerle, T., & Reid, I. N. 1996, *ApJ*, 464, 286
- Cieza, L. A., Schreiber, M. R., Romero, G. A., et al. 2012, *ApJ*, 750, 157
- Cohen, M., & Kuhl, L. V. 1979, *ApJS*, 41, 743
- Connelley, M. S., & Greene, T. P. 2010, *AJ*, 140, 1214
- Cowley, A. 1972, *AJ*, 77, 750
- Cruz, K. L., Kirkpatrick, J. D., & Burgasser, A. J. 2009, *AJ*, 137, 3345
- Cruz, K. L., Nunez, A., Burgasser, A. J., et al. *ApJ*, submitted
- Cruz, K. L., Reid, I. N., Kirkpatrick, J. D., et al. 2007, *AJ*, 133, 439
- Cushing, M. C., Rayner, J. T., & Vacca, W. D. 2005, *ApJ*, 623, 1115
- Cushing, M. C., Vacca, W. D., & Rayner, J. T. 2004, *PASP*, 116, 362
- Daemgen, S., Bonavita, M., Jayawardhana, R., Lafrenière, D., & Janson, M. 2015, *ApJ*, 799, 155
- DeWarf, L. E., Sepinsky, J. F., Guinan, E. F., Ribas, I., & Nadalin, I. 2003, *ApJ*, 590, 357
- Dobashi, K., Uehara, H., Kandori, R., et al. 2005, *PASJ*, 57, 1
- Doppmann, G. W., Greene, T. P., Covey, K. R., & Lada, C. J. 2005, *AJ*, 130, 1145
- Duchêne Monin, J.-L., Bouvier, J., & Ménard, F. 1999, *A&A*, 351, 954
- Ducourant, C., Teixeira, R., Périé, J. P., et al. 2005, *A&A*, 438, 769
- Esplin, T. L., Luhman, K. L., & Mamajek, E. E. 2014, *ApJ*, 784, 126
- Faherty, J. K., Rice, E. L., Cruz, K. L., Mamajek, E. E., & Núñez, A. 2013, *AJ*, 145, 2
- Faherty, J. K., Riedel, A. R., Cruz, K. L., et al. 2016, *ApJS*, 225, 10
- Fazio, G. G., Hora, J. L., Allen, L. E., et al. 2004, *ApJS*, 154, 10
- Feigelson, E. D., Jackson, J. M., Mathieu, R. D., Myers, P. C., & Walter, F. M. 1987, *AJ*, 94, 1251
- Feigelson, E. D., & Kriss, G. A., 1981, *ApJ*, 248, L35
- Feigelson, E. D., & Kriss, G. A., 1983, *AJ*, 88, 431
- Findeisen, K., & Hillenbrand, L. 2010, *AJ*, 139, 1338
- Finkbeiner, D. P., Padmanabhan, N., Schlegel, D. J., et al. 2004, *AJ*, 128, 2577
- Furlan, E., Luhman, K. L., Espaillat, C., et al. 2011, *ApJS*, 195, 3
- Gagné, J., Faherty, J. K., Cruz, K. L., et al. 2014, *ApJ*, 785, L14
- Gagné, J., Faherty, J. K., Cruz, K. L., et al. 2015, *ApJS*, 219, 33
- Gagné, J., et al. 2016, *ApJ*, submitted
- Gizis, J. E. 2002, *ApJ*, 575, 484
- Gomez, M., Jones, B. F., Hartmann, L., et al. 1992, *AJ*, 104, 762
- Gómez de Castro, A. I., Lopez-Santiago, J., López-Martínez, F., et al. 2015, *ApJS*, 216, 26
- Güdel, M., Briggs, K. R., Arzner, K., et al. 2007, *A&A*, 468, 353
- Guieu, S., Dougados, C., Monin, J.-L., Magnier, E. & Martín, E. L. 2006, *A&A*, 446, 485
- Harris, S. C., Peter, H., & Hughes, J. 1988, *MNRAS*, 235, 441
- Hartigan, P., Edwards, S., & Ghandour, L. 1995, *ApJ*, 452, 736
- Hartigan, P., & Kenyon, S. J. 2003, *ApJ*, 583, 334
- Hartigan, P., Strom, K. M., & Strom, S. E. 1994, *ApJ*, 427, 961
- Hartmann, L., Jones, B. F., Stauffer, J. R., & Kenyon, S. J. 1991, *AJ*, 101, 1050
- Henry, T. J., Kirkpatrick, J. D., & Simons, D. A. 1994, *AJ*, 108, 1437
- Herbig, G. H., Vrba, F. J., & Rydgren, A. E. 1986, *AJ*, 91, 575
- Herczeg, G. J., Cruz, K. L., & Hillenbrand, L. A. 2009, *ApJ*, 696, 1589
- Herczeg, G. J., & Hillenbrand, L. A. 2008, *ApJ*, 681, 594
- Herczeg, G. J., & Hillenbrand, L. A. 2014, *ApJ*, 786, 97
- Hillenbrand, L. A. 1997, *AJ*, 113, 1733
- Hillenbrand, L. A., & Carpenter, J. M. 2000, *ApJ*, 540, 236
- Hillenbrand, L. A., & Hartmann, L. W. 1998, *ApJ*, 492, 540
- Hodapp, K. W., Jensen, J. B., Irwin, E. M., et al. 2003, *PASP*, 115, 1388
- Hook, I., Jørgensen, I., Allington-Smith, J. R., et al. 2004, *PASP*, 116, 425
- Houk N. 1982, Michigan Catalogue of Two-dimensional Spectral Types for the HD Stars, Vol. 3, Declinations -40 (Ann Arbor, MI: Univ. Michigan), 12
- Itoh, Y., Hayashi, M., Tamura, M., et al. 2005, *ApJ*, 620, 984
- Jones, B. F., & Herbig, G. H. 1979, *AJ*, 84, 1872
- Joy, A. H. 1945, *ApJ*, 102, 168
- Joy, A. H. 1949, *ApJ*, 110, 424
- Kaiser, N., Aussel, H., Burke, B. E., et al. 2002, *Proc. SPIE*, 4836, 154
- Kastner, J. H., Zuckerman, B., & Bessell, M. 2008, *A&A*, 491, 829
- Kellogg, K., Metchev, S., Geißler, K., et al. 2015, *AJ*, 150, 182
- Kenyon, S. J., Brown, D. I., Tout, C. A., & Berlind, P. 1998, *AJ*, 115, 2491
- Kenyon, S. J., Gomez, M., Marzke, R., & Hartmann, L. 1994, *AJ*, 108, 251
- Kenyon, S. J., Gómez, M., & Whitney, B. A. 2008, *Handbook of Star Forming Regions*, Volume 1, ASP Monograph Series, 405
- Kenyon, S. J., & Hartmann, L. 1995, *ApJS*, 101, 117
- Kenyon, S. J., Hartmann, L. W., Strom, K. M., & Strom, S. E. 1990, *AJ*, 99, 869
- Kirkpatrick, J. D. 2005, *ARA&A*, 43, 195
- Kirkpatrick, J. D., Barman, T. S., Burgasser, A. J., et al. 2006, *ApJ*, 639, 1120
- Kirkpatrick, J. D., Gelino, C. R., Cushing, M. C., et al. 2012, *ApJ*, 753, 156
- Kirkpatrick, J. D., Henry, T. J., & Irwin, M. J. 1997, *AJ*, 113, 1421
- Kirkpatrick, J. D., Henry, T. J., & McCarthy, D. W. 1991, *ApJS*, 77, 417
- Kirkpatrick, J. D., Looper, D. L., Burgasser, A. J., et al. 2010, *ApJS*, 190, 100
- Kirkpatrick, J. D., Reid, I. N., Liebert, J., et al. 1999, *ApJ*, 519, 802
- Kohoutek, L., & Wehmeyer, R. 1999, *A&AS*, 134, 255
- Kraus, A. L., & Hillenbrand, L. A. 2009, *ApJ*, 703, 1511
- Lachapelle, F.-R., Lafrenière, D., Gagné, J., et al. 2015, *ApJ*, 802, 61
- Lafrenière, D., Jayawardhana, R., & van Kerkwijk, M. H. 2008, *ApJ*, 689, L153
- Lafrenière, D., Jayawardhana, R., & van Kerkwijk, M. H. 2010, *ApJ*, 719, 497

- Liu, M. C., Magnier, E. A., Deacon, N. R., et al. 2013, *ApJ*, 777, L20
- Lodieu, N., Hambly, N. C., Jameson, R. F., & Hodgkin, S. T. 2008, *MNRAS*, 383, 1385
- Loinard, L., Mioduszewski, A. J., Rodríguez, L. F., et al. 2005, *ApJ*, 619, L179
- Looper, D. L., Burgasser, A. J., Kirkpatrick, J. D., & Swift, B. J. 2007, *ApJ*, 669, L97
- Looper, D. L., Bochanski, J. J., Burgasser, A. J., et al. 2010b, *AJ*, 140, 1486
- Looper, D. L., Mohanty, S., & Bochanski, J. J., 2010a, *ApJ*, 714, 45
- Luhman, K. L. 1999, *ApJ*, 525, 466
- Luhman, K. L. 2000, *ApJ*, 544, 1044
- Luhman, K. L. 2004, *ApJ*, 617, 1216
- Luhman, K. L. 2006, *ApJ*, 645, 676
- Luhman, K. L. 2007, *ApJS*, 173, 104
- Luhman, K. L. 2012, *ARA&A*, 50, 65
- Luhman, K. L., Adame, L., D'Alessio, P., et al. 2007, *ApJ*, 666, 1219
- Luhman, K. L., Allen, P. R., Espaillat, C., Hartmann, L., & Calvet, N. 2010, *ApJS*, 186, 111
- Luhman, K. L., Briceño, C., Rieke, G. H., Hartmann, L. 1998, *ApJ*, 493, 909
- Luhman, K. L., Briceño, C., Stauffer, J. R., et al. 2003a, *ApJ*, 590, 348
- Luhman, K. L., Esplin, T. L., & Loutrel, N. P. 2016, *ApJ*, 827, 52
- Luhman, K. L., Mamajek, E. E., Allen, P. R., & Cruz, K. L. 2009b, *ApJ*, 703, 399
- Luhman, K. L., Mamajek, E. E., Allen, P. R., Muench, A. A., & Finkbeiner, D. P. 2009a, *ApJ*, 691, 1265
- Luhman, K. L., & Potter, D. 2006, *ApJ*, 638, 887
- Luhman, K. L., & Rieke, G. H. 1998, *ApJ*, 497, 354
- Luhman, K. L., Stauffer, J. R., Muench, A. A., et al. 2003b, *ApJ*, 593, 1093
- Luhman, K. L., Whitney, B. A., Meade, M. R., et al. 2006, *ApJ*, 647, 1180
- Malfait, K., Bogaert, E., & Waelkens, C. 1998, *A&A*, 331, 211
- Mamajek, E. E. 2005, *ApJ*, 634, 1385
- Martín, E. L. 2000, *AJ*, 120, 2114
- Martín, E. L., Dougados, C., Magnier, E., et al. 2001, *ApJ*, 561, L195
- Martín, E. L., & Magazzù, A. 1999, *A&A*, 342, 173
- Martín, E. L., Rebolo, R., Magazzù, A., & Pavlenko, Y. V. 1994, *A&A*, 282, 503
- Metchev, S. A., Kirkpatrick, J. D., Berriman, G. B., & Looper, D. 2008, *ApJ*, 676, 1281
- Meyer, M. R., Calvet, N., & Hillenbrand, L. A. 1997, *AJ*, 114, 288
- Mohanty, S., Stassun, K. G., & Mathieu, R. D. 2009, *ApJ*, 697, 713
- Monin, J.-L., Ménard, F., & Duchêne, G. 1998, *A&A*, 339, 113
- Mooley, K. P., Hillenbrand, L. A., Rebull, L., Padgett, D., & Knapp, G. 2013, *ApJ*, 771, 110
- Moraux, E., Kroupa, P., & Bouvier, J. 2004, *A&A*, 426, 75
- Muench, A. A., Lada, E. A., Lada, C. J., & Alves, J. 2002, *ApJ*, 573, 366
- Muench, A. A., Lada, E. A., Lada, C. J., et al. 2003, *AJ*, 125, 2029
- Muench, A. A., Lada, C. J., Luhman, K. L., Muzerolle, J., & Young, E. 2007, *AJ*, 134, 411
- Murphy, S. J., Lawson, W. A., & Bento, J. 2015, *MNRAS*, 453, 2220
- Muzerolle, J., Hillenbrand, L., Calvet, N., Briceño, C., & Hartmann, L. 2003, *ApJ*, 592, 266
- Myers, P. C., Fuller, G. A., Mathieu, R. D., et al. 1987, *ApJ*, 319, 340
- Naylor, T. 2009, *MNRAS*, 399, 432
- Nesterov, V. V., Kuzmin, A. V., Ashimbaeva, N. T., et al. 1995, *A&AS*, 110, 367
- Neuhäuser, R., Guenther, E. W., Petr, M. G., et al. 2000, *A&A*, 360, L39
- Neuhäuser, R., Sterzik, M. F., Schmitt, J. H. M. M., Wichmann, R., & Krautter, J. 1995, *A&A*, 295, L5
- Nguyen, D. C., Brandeker, A., VAn Kerkwijk, M. H., & Jawarwardhana, R. 2012, *ApJ*, 745, 119
- Padgett, D. L., Cieza, L., Stapelfeldt, K. R., et al. 2006, *ApJ*, 645, 1283
- Pecaut, M. J., & Mamajek, E. E. 2013, *ApJS*, 208, 9
- Perryman, M. A. C., de Boer, K. S., Gilmore, G., et al. 2001, *A&A*, 369, 339
- Prato, L., Lockhart, K. E., Johns-Krull, C. M., & Rayner, J. T. 2009, *AJ*, 137, 3931
- Prato, L., Simon, M., Mazeh, T., Zucker, S., & McLean, I. S. 2002, *ApJ*, 579, L99
- Rayner, J. T., Cushing, M. C., & Vacca, W. D. 2009, *ApJS*, 185, 289
- Rayner, J. T., Toomey, D. W., Onaka, P. M., et al. 2003, *PASP*, 115, 362
- Rebull, L. M., Koenig, X. P., Padgett, D. L., et al. 2011, *ApJS*, 196, 4
- Rebull, L. M., Padgett, D. L., McCabe, C. E., et al. 2010, *ApJS*, 186, 259
- Reid, I. N. 2003, *MNRAS*, 342, 837
- Reid, I. N., Cruz, K. L., Kirkpatrick, J. D., et al. 2008, *AJ*, 136, 1290
- Reid, I. N., Gizis, J. E., & Hawley, S. L. 2002, *AJ*, 124, 2721
- Reid, I. N., & Hawley, S. L. 1999, *AJ*, 117, 343
- Riedel, A. R., Finch, C. T., Henry, T. J., et al. 2014, *AJ*, 147, 85
- Reiners, A., Seifahrt, A., Stassun, K. G., Melo, C., & Mathieu, R. D. 2007, *ApJ*, 761, L149
- Roeser, S., Demleitner, M., & Schilbach, E. 2010, *AJ*, 139, 2440
- Scelsi, L., Maggio, A., Micela, G., et al. 2007, *A&A*, 468, 405
- Scelsi, L., Sacco, G., Affer, L., et al. 2008, *A&A*, 490, 601
- Schaefer, G. H., Dutrey, A., Guilloteau, S., Simon, M., & White, R. J. 2009, *ApJ*, 701, 698
- Schneider, A., Song, I., Melis, C., Zuckerman, B., & Bessell, M. 2012, *ApJ*, 757, 163
- Schneider, A. C., Windsor, J., Cushing, M. C., Kirkpatrick, J. D., & Wright, E. L. 2016, *ApJ*, 822, L1
- Scholz, R.-D., McCaughrean, M. J., Zinnecker, H., & Lodieu, N. 2005, *A&A*, 430, L49
- Sestito, P., Palla, F., & Randich, S. 2008, *A&A*, 487, 965
- Shkolnik, E. L., Liu, M. C., Reid, I. N., Dupuy, T., & Weinberger, A. J. 2011, *ApJ*, 727, 6
- Skrutskie, M., Cutri, R. M., Stiening, R., et al. 2006, *AJ*, 131, 1163
- Slesnick, C. L., Carpenter, J. M., Hillenbrand, L. A., & Mamajek, E. E. 2006, *AJ*, 132, 2665
- Soderblom, D. R., Jones, B. F., Balachandran, S., et al. 1993, *AJ*, 106, 1059
- Stassun, K. G., Kratter, K., Scholz, A., & Dupuy, T. J. 2012, *ApJ*, 756, 47
- Stassun, K. G., Mathieu, R. D., & Valenti, J. A. 2006, *Nature*, 440, 311
- Stassun, K. G., Mathieu, R. D., & Valenti, J. A. 2007, *ApJ*, 664, 1154
- Stassun, K. G., Scholz, A., Dupuy, T. J., & Kratter, K. M. 2014, *ApJ*, 796, 119
- Steffen, A. T., Mathieu, R. D., Lattanzi, M. G., et al. 2001, *AJ*, 122, 997
- Sterzik, M. F., Alcalá, J. M., Covino, E., & Petr, M. G. 1999, *A&A*, 346, L41
- Strom, K. M., & Strom, S. E. 1994, *ApJ*, 424, 237
- Torres, R. M., Loinard, L., Mioduszewski, A. J., et al. 2007, *ApJ*, 671, 1813
- Torres, R. M., Loinard, L., Mioduszewski, A. J., et al. 2009, *ApJ*, 698, 242
- Torres, R. M., Loinard, L., Mioduszewski, A. J., et al. 2012, *ApJ*, 747, 18
- Torres, C. A. O., da Silva, L., Quast, G. R., de la Reza, R., & Jilinski, E. 2000, *AJ*, 120, 1410
- Torres, C. A. O., Quast, G. R., da Silva, L., et al. 2006, *A&A*, 460, 695
- Torres, C. A. O., Quast, G., de la Reza, R., Gregorio-Hetem, J., Lepine, J. R. D. 1995, *AJ*, 109, 2146
- Vacca, W. D., Cushing, M. C., & Rayner, J. T., 2003, *PASP*, 115, 389
- Vacca, W. D., & Sandell, G. 2011, *ApJ*, 732, 8
- Walter, F. M., Beck, T. L., Morse, J. A., & Wolk, S. J. 2003, *AJ*, 125, 2123
- Walter, F. M., Brown, A., Mathieu, R. D., Myers, P. C., & Vrba, F. J. 1988, *AJ*, 96, 297
- Walter, F. M., & Kuhi, L. V. 1981, *ApJ*, 250, 254
- Webb, R. A., Zuckerman, B., Platais, I., et al. 1999, *ApJ*, 512, L63

- Welty, A. D. 1995, *AJ*, 110, 776
- Werner, M. W., Roellig, T. L., Low, F. J., et al. 2004, *ApJS*, 154, 1
- White, R. J., & Basri, G. 2003, *ApJ*, 582, 1109
- White, R. J., & Ghez, A. M. 2001, *ApJ*, 556, 265
- White, R. J., Ghez, A. M., Reid, I. N., & Schultz, G. 1999, *ApJ*, 520, 811
- White, R. J., & Hillenbrand, L. A. 2004, *ApJ*, 616, 998
- Wichmann, R., Bastian, U., Krautter, J., Jankovics, I., & Ruciński, S. M. 1998, *MNRAS*, 301, L39
- Wichmann, R., Krautter, J., Schmitt, J. H. M. M., et al. 1996, *A&A*, 312, 439
- Wichmann, R., Torres, G., Melo, C. H. F., et al. 2000, *A&A*, 359, 181
- Wu, Y.-L., Close, L. M., Males, J. R., et al. 2015, *ApJ*, 807, L13
- Wright, E. L., Eisenhardt, P. R. M., Mainzer, A. K., et al. 2010, *AJ*, 140, 1868
- York, D. G., Adelman, J., Anderson, J. E., et al. 2000, *AJ*, 120, 1579
- Zacharias, N., Finch, C. T., Girard, T. M., et al. 2013, *AJ*, 145, 44
- Zuckerman, B., & Song, I. 2004, *ARA&A*, 42, 685
- Zuckerman, B., Webb, R. A., Schwartz, M., & Becklin, E. E. 2001, *ApJ*, 549, L233

TABLE 1
MEMBERS OF TAURUS

Column Label	Description
2MASS	2MASS Point Source Catalog source name
WISE	WISE All Sky Source Catalog source name ^a
RAh	Hour of Right Ascension (J2000)
RAm	Minute of Right Ascension (J2000)
RAs	Second of Right Ascension (J2000)
DEd	Degree of Declination (J2000)
DEm	Arcminute of Declination (J2000)
DEs	Arcsecond of Declination (J2000)
Name	Source name
SpType	Spectral type
r_SpType	Spectral type reference ^b
Adopt	Adopted spectral type
Spexdate	SpeX date
A _J	Extinction in <i>J</i>
f_A _J	Method of extinction estimation ^c

NOTE. — The table is available in a machine-readable form.

^a Source names for HBC 360, HBC 361, and IRAM 04191+1522 are from the ALLWISE Source Catalog.

^b (1) Hartigan & Kenyon (2003); (2) Herczeg & Hillenbrand (2014); (3) Luhman et al. (2009b); (4) Kenyon & Hartmann (1995); (5) White & Hillenbrand (2004); (6) Doppmann et al. (2005); (7) Prato et al. (2009); (8) Esplin et al. (2014); (9) Wichmann et al. (1996); (10) Nguyen et al. (2012); (11) Luhman (2006); (12) this work; (13) Findeisen & Hillenbrand (2010); (14) Connelley & Greene (2010); (15) Torres et al. (1995); (16) Schaefer et al. (2009); (17) Rebull et al. (2010); (18) Luhman (2004); (19) Welty (1995); (20) White & Basri (2003); (21) Briceño et al. (1998); (22) Strom & Strom (1994); (23) Scelsi et al. (2008); (24) Briceño et al. (2002); (25) Guieu et al. (2006); (26) Slesnick et al. (2006); (27) Luhman & Rieke (1998); (28) Luhman et al. (2003a); (29) Luhman et al. (1998); (30) Martín et al. (2001); (31) Hartigan et al. (1994); (32) Kenyon et al. (1998); (33) Beck (2007); (34) Luhman (1999); (35) Calvet et al. (2004); (36) Reid & Hawley (1999); (37) Luhman et al. (2006); (38) Cieza et al. (2012); (39) Duchêne et al. (1999); (40) White & Ghez (2001); (41) Bonnefoy et al. (2014); (42) Itoh et al. (2005); (43) Monin et al. (1998); (44) Muzerolle et al. (2003); (45) Kraus & Hillenbrand (2009); (46) White et al. (1999); (47) Martín & Magazzù (1999); (48) Prato et al. (2002); (49) Walter et al. (2003); (50) Cowley (1972); (51) Martín et al. (1994); (52) Herczeg & Hillenbrand (2008); (53) Nesterov et al. (1995); (54) Martín (2000); (55) Bowler & Hillenbrand (2015); (56) Briceño et al. (1999); (57) Hartigan et al. (1995); (58) Cohen & Kuhl (1979); (59) Boss (1937); (60) Steffen et al. (2001); (61) Malfait et al. (1998); (62) Briceño et al. (1993).

^c $J - H$ and $J - K$ = derived from these colors assuming photospheric near-IR colors; CTTS = derived from $J - H$ and $H - K$ assuming intrinsic colors of classical T Tauri stars from Meyer et al. (1997); opt spec = derived from an optical spectrum; SpeX = derived from a SpeX spectrum; (1) = Briceño et al. (1998); (2) = Luhman (2000); (3) = Strom & Strom (1994); (4) = Beck (2007); (5) = White & Ghez (2001); (6) = DeWarf et al. (2003); (7) = Calvet et al. (2004).

TABLE 2
NEW MEMBERS OF TAURUS IN SPECTROSCOPIC SAMPLE

2MASS	Spectral Type	Basis of Selection ^a	Telescope & Instrument	Date
J04105425+2501266	M1-M3	IR	Gemini/NIRI	2009 Dec 26
J04144158+2809583	M9.75	WIRCam/IRAC	IRTF/SpeX	2013 Jan 3
J04153452+2913469	K-M+?	IR	Gemini/NIRI	2009 Dec 7
J04153566+2847417	M4.5-M6.5	IR	IRTF/SpeX	2010 Jan 3
J04154131+2915078	M5.75	CMDs	IRTF/SpeX	2010 Jan 3
J04154269+2909558 ^b	M6.5	companion?	HET/LRS	2009 Nov 8
J04154807+2911331	M9	CMDs	IRTF/SpeX	2010 Jan 3
J04161726+2817128	M4.75	CMDs	IRTF/SpeX	2010 Jan 16
J04213965+2649143	M6	CMDs	IRTF/SpeX	2010 Jan 3
J04215482+2642372	M5	CMDs	IRTF/SpeX	2010 Jan 4
J04245021+2641006	M5	CMDs	IRTF/SpeX	2010 Jan 4
J04264449+2756433	M6	CMDs	IRTF/SpeX	2010 Jan 4
J04272467+2624199	M3	CMDs	IRTF/SpeX	2010 Jan 16
J04314644+2506236	M5.5	CMDs	IRTF/SpeX	2010 Jan 4
J04340619+2418508	M8.25	CMDs	IRTF/SpeX	2010 Jan 3
J04344586+2445145	M4.75	CMDs	IRTF/SpeX	2010 Dec 23
J04345973+2807017	M5.75	IR	HET/LRS	2009 Nov 8
J04351316+1725496	M4.5,M4	pm	HET/LRS,IRTF/SpeX	2009 Dec 26,2010 Jan 3
J04355881+2438404	M3	CMDs	IRTF/SpeX	2010 Jan 16
J04363248+2421395	M8	CMDs	IRTF/SpeX	2010 Jan 4
J04590305+3003004	M2	H α ,X-ray,pm	HET/LRS	2009 Dec 26
J05000310+3001074 ^c	M1.5+?	H α ,IR,pm	HET/LRS,IRTF/SpeX	2009 Dec 26,2010 Jan 3

^a Sources were selected for spectroscopy because they were candidate members based on possible companionship to known Taurus members, CMDs, X-ray emission, H α emission, mid-IR excess emission, proper motions (“pm”), or red WIRCam/IRAC colors.

^b Candidate companion to IRAS 04125+2902.

^c GZ Aur A and B. Both components were observed by SpeX. Only the primary was observed by LRS.

TABLE 3
NONMEMBERS IN SPECTROSCOPIC SAMPLE

Name	Spectral Type	Basis of Selection ^a	Telescope & Instrument	Date
2MASS J04130959+2440204	M5V	CMDs	IRTF/SpeX	2010 Dec 23
2MASS J04155686+2907509	galaxy	IR	Gemini/GMOS	2009 Oct 20
2MASS J04162497+3037545	L1.5V	CMDs	IRTF/SpeX	2010 Jan 3
2MASS J04181059+2844473	galaxy	IR	Gemini/GMOS	2009 Oct 22
2MASS J04181375+2539395	M6V	CMDs	IRTF/SpeX	2010 Jan 4
2MASS J04182560+2836371	F	CMDs	IRTF/SpeX	2010 Jan 4
2MASS J04224036+2441144	giant	CMDs	IRTF/SpeX	2010 Dec 23
2MASS J04232153+2453513	giant	CMDs	IRTF/SpeX	2010 Dec 23
2MASS J04234043+2844151	M7V	CMDs	IRTF/SpeX	2010 Dec 23
2MASS J04263650+2439469	giant	CMDs	IRTF/SpeX	2010 Dec 23
2MASS J04264776+2456594	M4.5V	CMDs	IRTF/SpeX	2010 Jan 4
2MASS J04280370+2424077	M5V	CMDs	IRTF/SpeX	2010 Dec 23
WISE J042823.04+264933.8	galaxy	IR	Gemini/NIRI	2009 Oct 1
2MASS J04305575+2450174	M4.5V	CMDs	IRTF/SpeX	2010 Jan 4
WISE J043809.73+254731.5	galaxy	IR	Gemini/NIRI	2009 Oct 4
2MASS J04381659+2614500	giant	CMDs	IRTF/SpeX	2010 Dec 23
2MASS J04435167+2519576	M3.5V	CMDs	IRTF/SpeX	2010 Dec 23
2MASS J04511884+2556333	M5V	CMDs	IRTF/SpeX	2010 Jan 4

^a Sources were selected for spectroscopy because they were candidate members based on CMDs or mid-IR excess emission.

TABLE 4
SPECTRAL TYPES FOR KNOWN MEMBERS OF TWA

TWA ^a	2MASS	Other Names	Spectral Type ^b	Ref	Adopt
1	J11015191–3442170	TW Hya	K7,K8,K6,M2.5(ir),K8,M0.5,M1	1,2,3,4,5,6,7	M1
2	J11091380–3001398	CD–29 8887	M0.5,M2,M2,M1.5,M1.5,M2.2,M2.25	1,2,3,8,5,6,7	M2.25
3A	J11102788–3731520	Hen 3-600 A	M3,M4,M4,M3.9,M4,M4.1,M4.25	1,2,3,8,5,6,7	M4.25
3B	J11102788–3731520	Hen 3-600 B	M3.5,M4,M3.9,M4,M4.25	1,3,8,6,7	M4.25
4	J11220530–2446393	HD 98800	K5,K7,K5,K6,K6,K7	1,2,3,5,6,7	K6.5
5A	J11315526–3436272	CD–33 7795	M1.5,M3,M2,M1.9,M2,M2.7,M3	1,2,3,8,5,6,7	M3
5B	M8.75,M8.5(ir)	9,10	M8.5
6	J10182870–3150029	Tyc 7183-1477-1	K7,M0,M0,M0	1,3,6,7	M0
7	J10423011–3340162	Tyc 7190-2111-1	M1,M2,M3,M3.2,M3.25	1,3,5,6,7	M3.25
8A	J11324124–2651559	GSC 06659-01080	M2,M2,M3,M2.4,M3,M2.9,M3.25	1,2,3,8,5,6,7	M3.25
8B	J11324116–2652090	...	M5,M5.2,M5.5	1,6,7	M5.25
10	J12350424–4136385	GSC 0776-00743	M2.5,M2,M2.6,M3.25	1,3,8,7	M3
11A	J12360103–3952102	HR 4796 A	A0	1	A0
11B	...	HR 4796 B	M2.5	1	M2.5
11C	J12354893–3950245	HR 4796 C	M4.5,M4.5,M5(ir)	11,7,12	M4.5
12	J11210549–3845163	RX J1121.1–3845	M1.5,M1.6,M2,M2.75	3,8,5,7	M2.75
13A	J11211723–3446454	RX J1121.3–3447	M2,M1,M1.1,M1	13,3,6,7	M1
13B	J11211745–3446497	...	M1	13,3,6	M1
16	J12345629–4538075	UCAC2 12217020	M1.5,M1.8,M2,M3	14,8,5,7	M3
20	J12313807–4558593	GSC 08231-02642	M2,M3,M3.25	15,5,7	M3.25
21	J10131476–5230540	HD 298936	K3/K4,K3,K3	16,3,5	K3
23	J12072738–3247002	SSSPM 1207–3247	M1,M2.9,M3.5	16,8,7	M3.5
25	J12153072–3948426	Tyc 7760-283-1	M0,M1,K9,M0.5,M0.75	16,3,5,6,7	M0.75
26	J11395113–3159214	...	M8,M9(ir),M9,M9(ir),M8.5	17,18,19,12,7	M8.5
27A	J12073346–3932539	...	M8,M8(ir),M8.25,M8.5(ir),M8(ir),M8.5(ir)	17,18,20,10,12,21	M8.25
27B	L3(ir)	12	mid L
28	J11020983–3430355	SSSPM 1102–3431	M8.5,M9(ir),M8.5	22,12,6	M8.5
29	J12451416–4429077	DENIS 1245–4429	M9.5,M9(ir),M9.25	18,18,7	M9.25
30A	J11321831–3019518	...	M5,M4.75	23,7	M4.75
30B	J11321822–3018316	...	M4	24	M4
32	J12265135–3316124	...	M6.3,M5.25	8,7	M5.25
33	J11393382–3040002	...	M4.7,M4.75	25,7	M4.75
34	J10284580–2830374	...	M4.9,M5.5	25,7	M5.5
35	J12002750–3405371	...	M4.7	26	M4.7
36	J12023799–3328402	...	M4.8	26	M4.8
39	J10120908–3124451	SCR 1012–3124 AB	M4	27	M4
40	J12074836–3900043	...	L0,L1(ir),L1(ir),M9.5(ir)	28,28,21,7	M9.75
41	J11472421–2040204	WISEA 1147–2040	L7(ir)	29	L7
42	J11193254–1137466	...	L7(ir)	30	L7
43	J11084400–2804504	HIP 54477	A1	31	A1

REFERENCES. — (1) Webb et al. (1999); (2) Torres et al. (2000); (3) Torres et al. (2006); (4) Vacca et al. (2011); (5) Pecaut & Mamajek (2013); (6) Herczeg & Hillenbrand (2014); (7) this work; (8) Shkolnik et al. (2011); (9) Neuhäuser et al. (2000); (10) Bonnefoy et al. (2014); (11) Kastner et al. (2008); (12) Allers & Liu (2013); (13) Sterzik et al. (1999); (14) Zuckerman et al. (2001); (15) Reid (2003); (16) Zuckerman & Song (2004); (17) Gizis (2002); (18) Looper et al. (2007); (19) Reid et al. (2008); (20) Herczeg et al. (2009); (21) Gagné et al. (2015); (22) Scholz et al. (2005); (23) Looper et al. (2010a); (24) Looper et al. (2010b); (25) Schneider et al. (2012); (26) Murphy et al. (2015); (27) Riedel et al. (2014); (28) Gagné et al. (2014); (29) Schneider et al. (2016); (30) Kellogg et al. (2015); (31) Houk et al. (1982).

^a TWA names 39 through 43 were assigned by Gagné et al. (2016).

^b Spectral types measured from near-IR spectra are indicated by “ir”.

TABLE 5
DATA FOR CONSTRUCTION OF STANDARD SPECTRA

Name	Spectral Type	Ref	SpeX Date	Ref
TWA 6	M0	1	2005 Dec 14	2
TWA 1	M1	1	2005 Dec 14	2
TWA 13	M1	1	2011 Dec 3	2
UX Tau B	M2	3	2008 Nov 2	2
TWA 2	M2.25	1	2005 Dec 14	2
TWA 12	M2.75	1	2015 Apr 20	2
DM Tau	M3	3	2008 Nov 2	2
TWA 10	M3	1	2015 Apr 21	2
TWA 7	M3.25	1	2005 Dec 14	2
TWA 8A	M3.25	1	2005 Dec 14	2
LRL 85	M3.25	4	2004 Nov 12	6
TWA 23	M3.5	1	2015 Apr 19	2
LRL 147	M3.5	4	2004 Nov 12	6
MHO 9	M4.25	3	2004 Nov 11	6
2MASS J04351316+1725496	M4.5	3	2010 Jan 3	2
TWA 11C	M4.5	1	2015 Apr 22	2
2MASS J04554757+3028077	M4.75	3	2004 Nov 12	6
TWA 33	M4.75	1	2015 Apr 19	2
2MASS J16160602-2528217	M4.75	7	2013 Jun 21	2
KPNO 10	M5	3	2004 Nov 11	6
Haro 6-32	M5	3	2004 Nov 12	6
2MASS J04555288+3006523	M5.25	3	2004 Nov 12	6
MHO 7	M5.25	3	2004 Nov 11	6
TWA 8B	M5.25	1	2005 Dec 14	2
TWA 32	M5.25	1	2015 Apr 21	2
TWA 34	M5.5	1	2015 Apr 20	2
2MASS J16134045-2233156	M5.5	7	2012 Apr 25	2
2MASS J16002631-2259412	M5.5	7	2006 Jun 15	2
TWA 37	M5.75	1	2015 Apr 20	2
FW Tau	M5.8	3	2008 Nov 2	2
MHO 8	M6	3	2004 Nov 12	6
V410 X-ray 3	M6.25	3	2004 Nov 11	6
2MASS J04552333+3027366	M6.25	3	2004 Nov 12	6
2MASS J16051403-2406524	M6.5	7	2005 Jun 16	2
2MASS J16095852-2345186	M6.5	7	2005 Jun 16	2
MHO 4	M7	3	2004 Nov 11	6
CFHT 4	M7	3	2004 Nov 11	6
FU Tau A	M7	3	2007 Dec 3	8
2MASS J16114261-2525511	M7	7	2013 Jun 21	2
2MASS J04390396+2544264	M7.25	3	2004 Nov 11	6
KPNO 2	M7.5	3	2004 Nov 11	6
KPNO 5	M7.5	3	2004 Nov 11	6
CFHT 3	M7.75	3	2004 Nov 11	6
2MASS J04414825+2534304	M7.75	3	2004 Nov 11	6
LRL 405	M8	5	2004 Nov 12	6
KPNO 7	M8.25	3	2004 Nov 11	6
2MASS J04290068+2755033	M8.25	3	2005 Dec 14	2
LH 0429+17	M8.25	3	2007 Dec 3	9
TWA 27	M8.25	1	2007 Mar 16,2015 Dec 14	10,2
KPNO 6	M8.5	3	2004 Nov 11	6
KPNO 1	M8.5	3	2004 Nov 11	6
TWA 26	M8.5	1	2005 Dec 14	2
TWA 28	M8.5	1	2005 Dec 14	2
2MASS J04263055+2443558	M8.75	3	2004 Nov 13	11
2MASS J04334291+2526470	M8.75	3	2005 Dec 13	11
KPNO 12	M9	3	2004 Nov 11	6
2MASS J04574903+3015195	M9.25	3	2004 Nov 11	6
TWA 29	M9.25	1	2007 Mar 17	10
KPNO 4	M9.5	3	2004 Nov 11	6
2MASS J01415823-4633574	L0	12	2004 Sep 4	13
2MASS J22134491-2136079	L0	12	2011 Sep 7	14
2MASS J23153135+0617146	L0	15	2007 Nov 13	16
2MASS J00550564+0134365	L2	15	2003 Sep 3	16
2MASS J05361998-1920396	L2	17	2012 Sep 19	14
2MASS J05012406-0010452	L4	18,12	2010 Jan 3	2
2MASS J01262109+1428057	L4	17	2006 Dec 7	19
TWA 41	L7	1	2016 Feb 11	20
TWA 42	L7	1	2013 Jun 5-6	21

REFERENCES. — (1) Table 4; (2) this work; (3) Table 1; (4) Luhman et al. (2003b); (5) Luhman (1999); (6) Muench et al. (2007); (7) K. Luhman, in preparation; (8) Luhman et al. (2009a); (9) Luhman et al. (2009b); (10) Looper et al. (2007); (11) Luhman (2006); (12) Cruz et al. (2009); (13) Kirkpatrick et al. (2006); (14) Allers & Liu (2013); (15) Cruz et al. (2016); (16) Faherty et al. (2016); (17) Faherty et al. (2013); (18) Reid et al. (2008); (19) Metchev et al. (2008); (20) Schneider et al. (2016); (21) Kellogg et al. (2015).

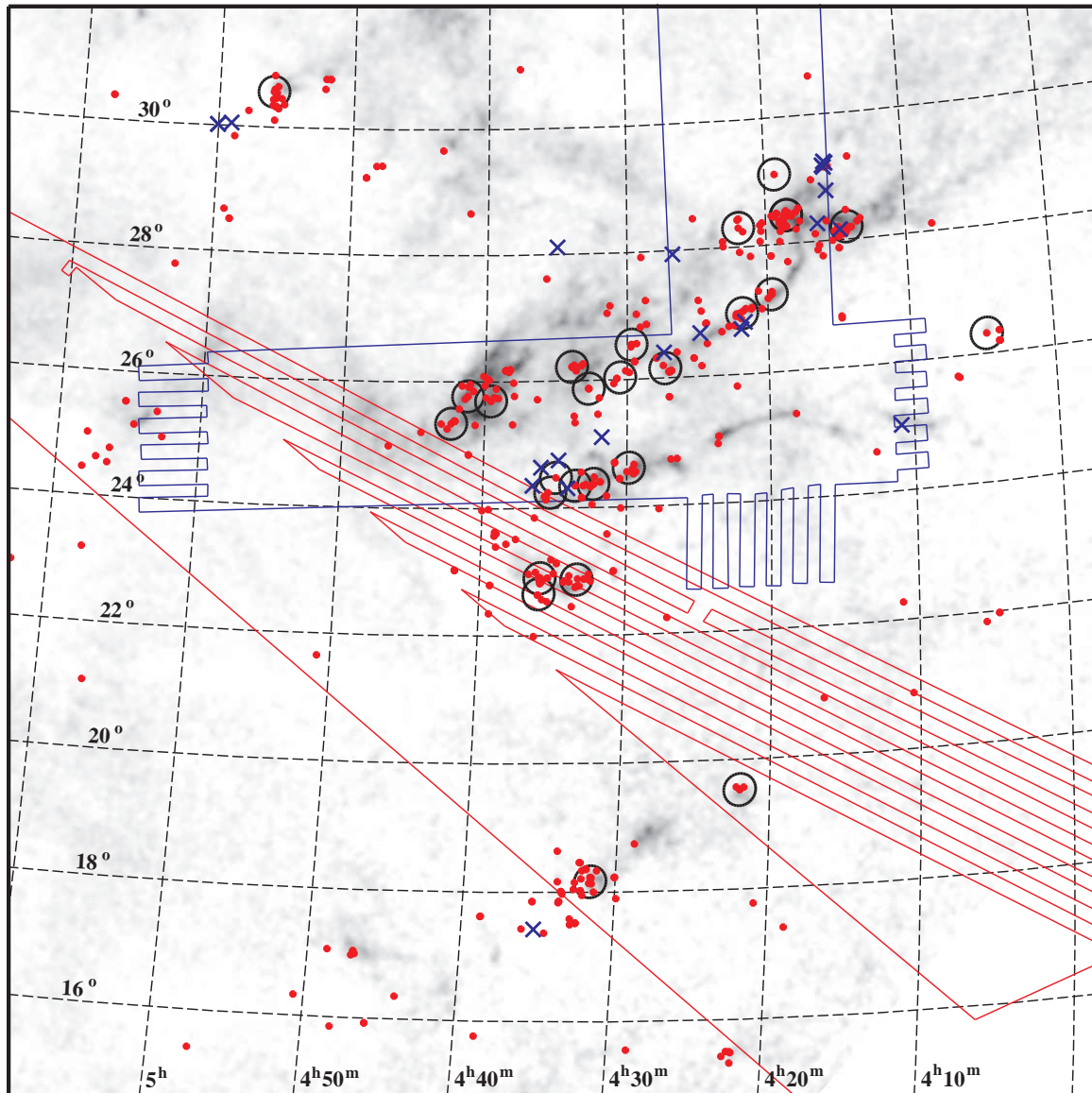


FIG. 1.— Spatial distribution of previously known members of the Taurus star-forming region (filled circles) and new members from this work (crosses). The field enclosed by the blue lines was imaged by SDSS in Finkbeiner et al. (2004). Most of the new members were identified as candidates with photometry from SDSS and 2MASS in that field. After the observations in Finkbeiner et al. (2004), SDSS observed additional areas that are outlined with the red lines. The fields imaged with *XMM-Newton* through the XEST program are indicated (large circles, Güdel et al. 2007). The dark clouds in Taurus are displayed with a map of extinction (gray scale, Dobashi et al. 2005).

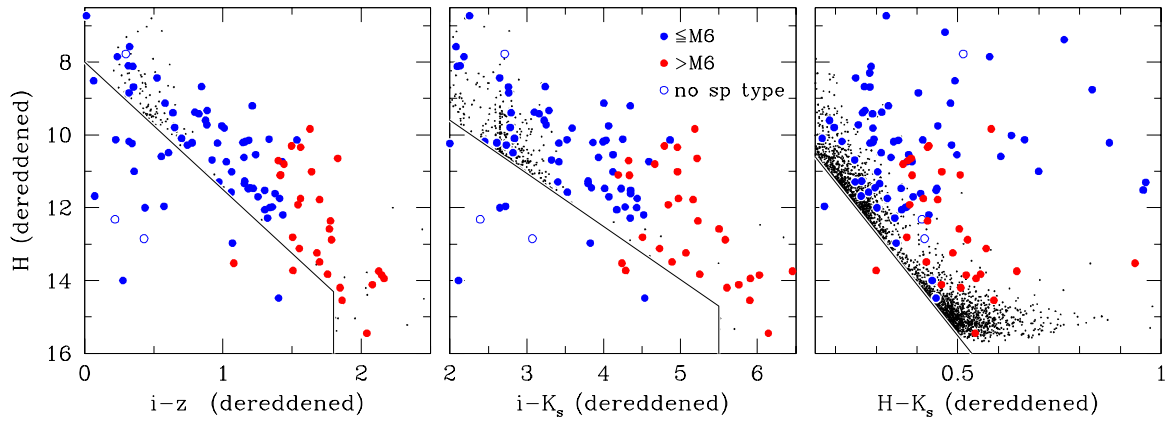


FIG. 2.— Extinction-corrected CMDs from SDSS and 2MASS for the known members of Taurus (large filled circles) and other sources (small points) that are within the SDSS field from Finkbeiner et al. (2004) (Figure 1). Candidate members have been selected based on positions above the solid boundaries. Stars below the boundaries have been omitted for clarity.

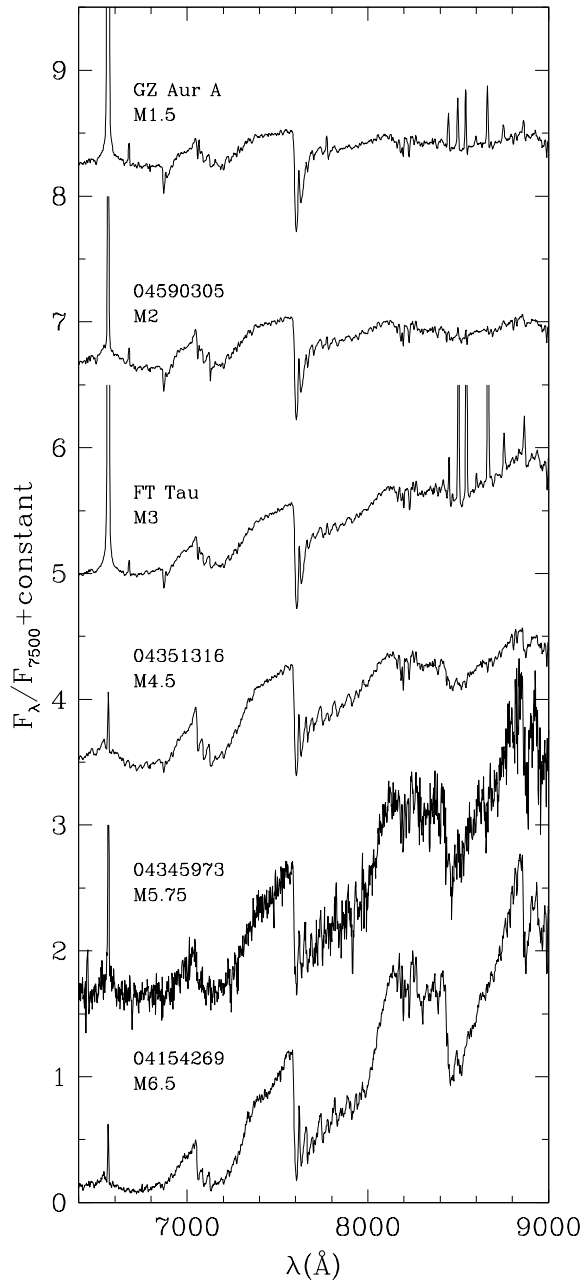


FIG. 3.— Optical spectra of new and previously known members of Taurus. The spectral types measured from these data are indicated. The spectra have a resolution of 7 Å. The data used to create this figure are available.

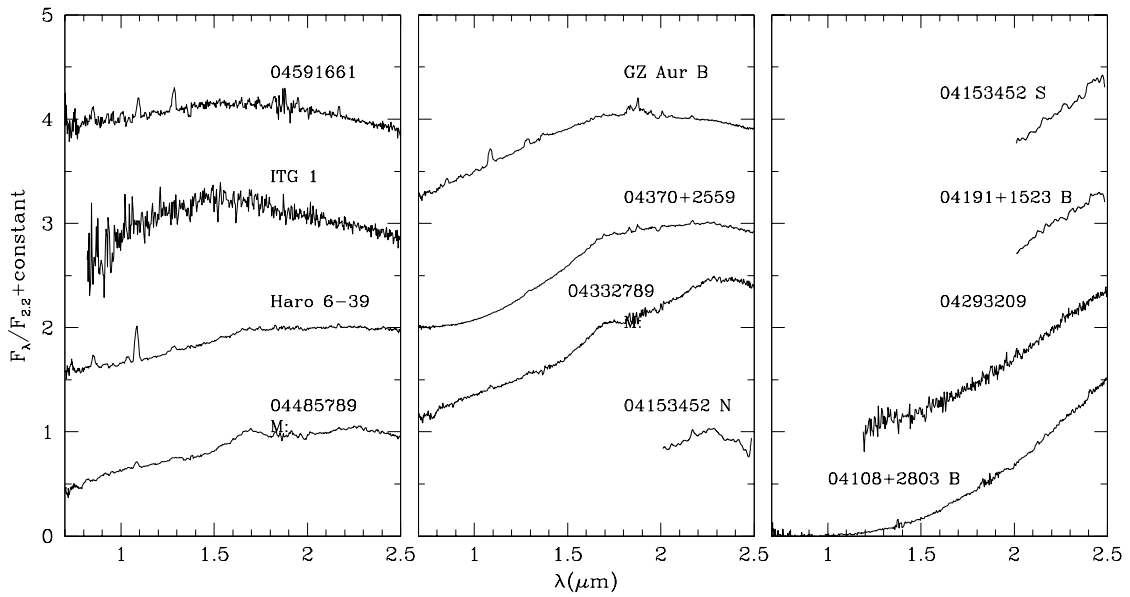


FIG. 4.— Near-IR spectra of members of Taurus that lack measured spectral types (Luhman et al. 2006, 2009b; Esplin et al. 2014, this work). These data have a resolution of $R = 150$. The data used to create this figure are available.

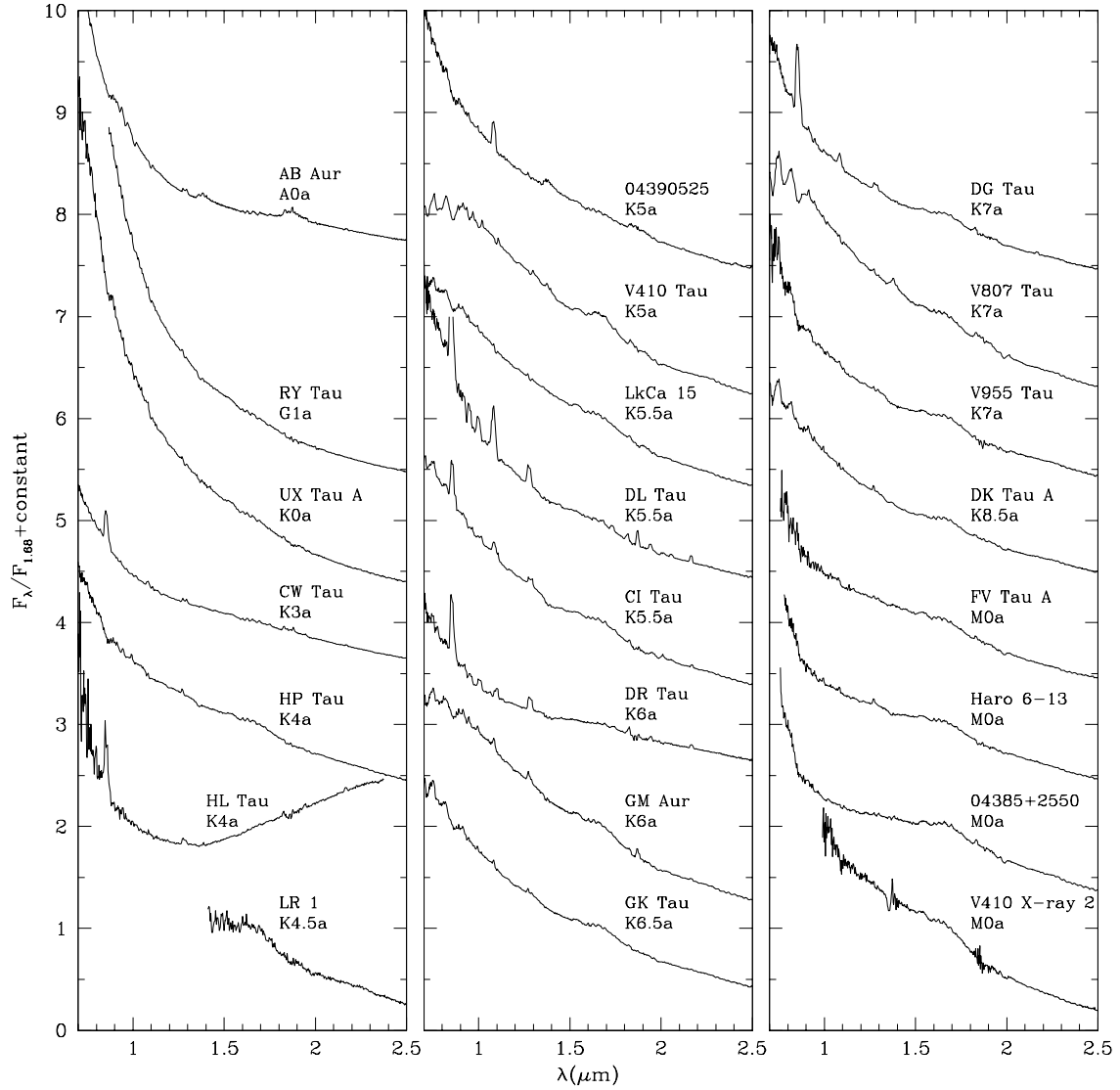


FIG. 5.— Near-IR spectra of members of Taurus (Luhman 2006; Luhman et al. 2006, 2007, 2009a,b; Muench et al. 2007; Esplin et al. 2014, this work). The spectral types denoted with “a” have been adopted from optical spectra because accurate types could not be measured from these IR data or the objects serve as standards for classifying our IR spectra (see Appendix). The remaining types have been measured from these spectra. The spectra have been dereddened to match the slopes of standards near $1 \mu\text{m}$. These data have a resolution of $R = 150$. The data used to create this figure are available.

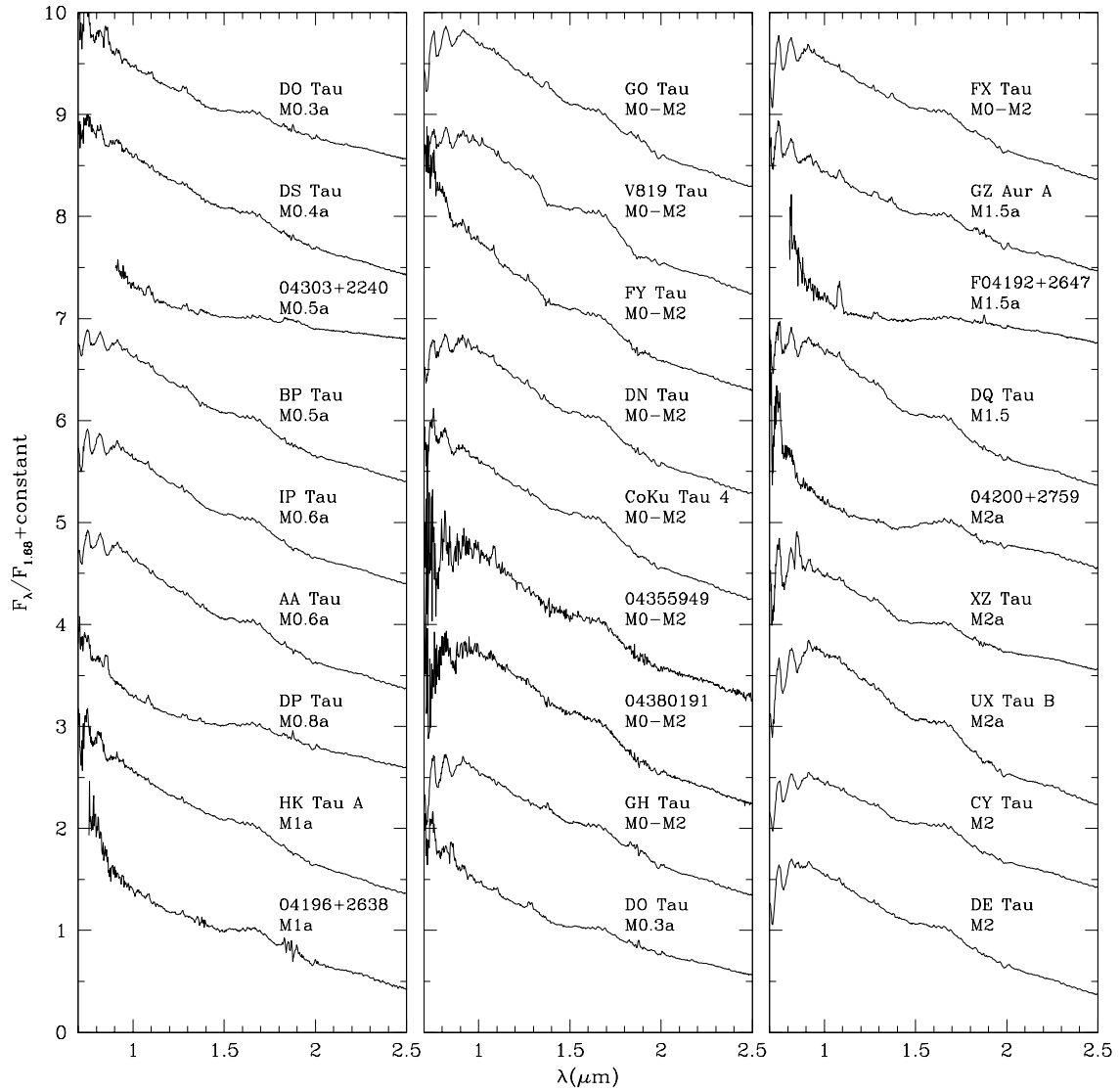


FIG. 6.— More near-IR spectra of members of Taurus (see Figure 5). The data used to create this figure are available.

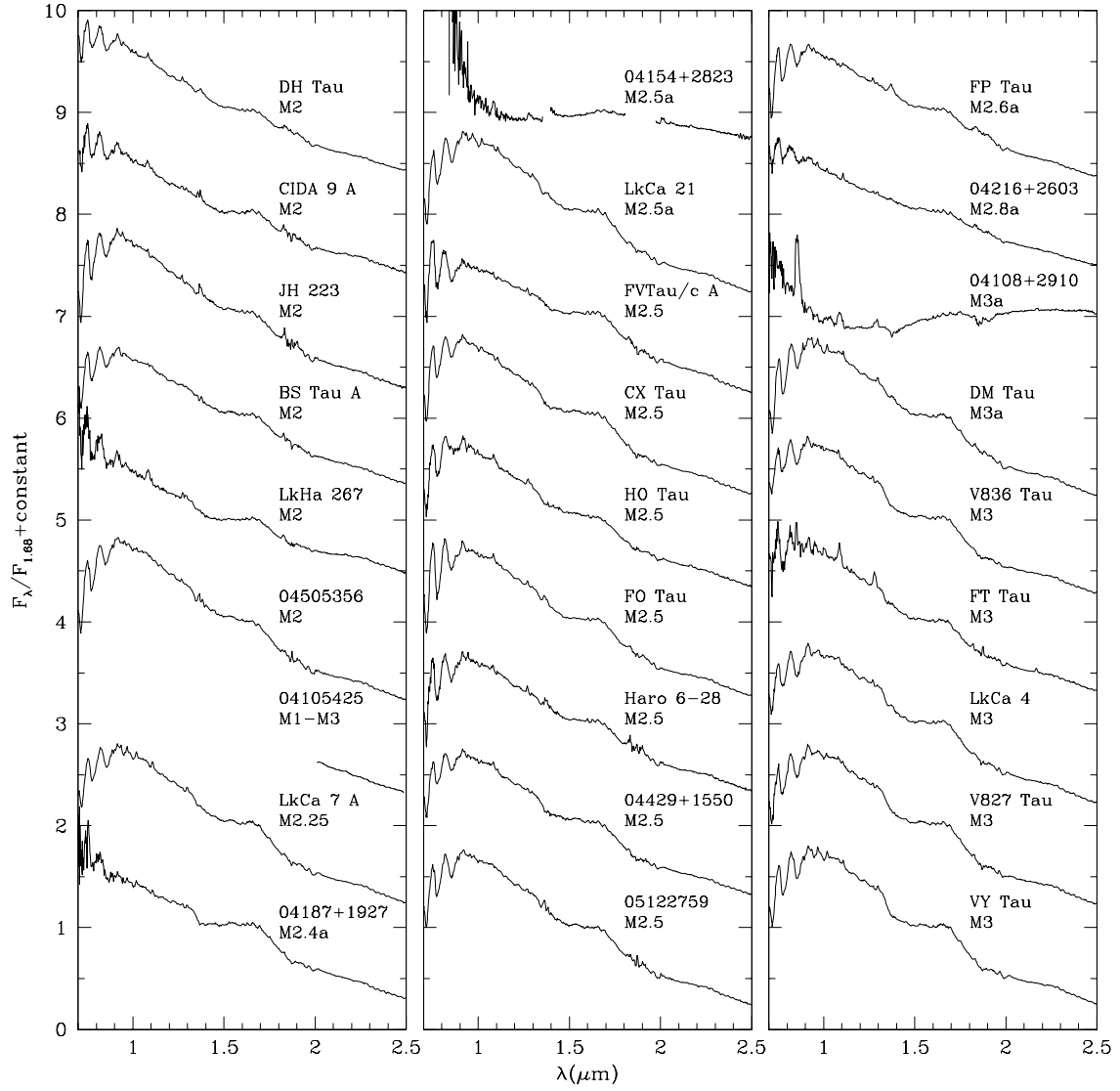


FIG. 7.— More near-IR spectra of members of Taurus (see Figure 5). The data used to create this figure are available.

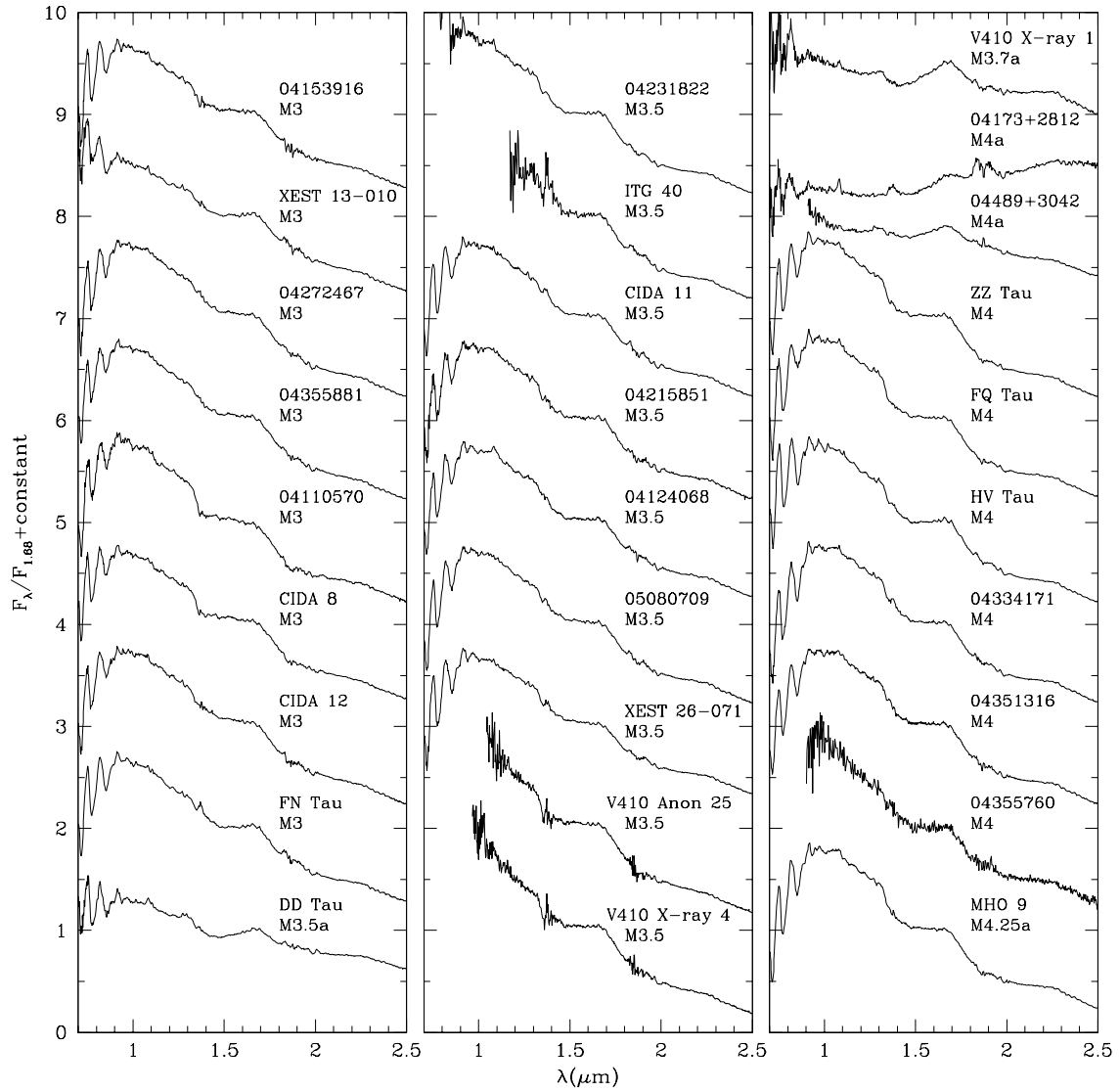


FIG. 8.— More near-IR spectra of members of Taurus (see Figure 5). The data used to create this figure are available.

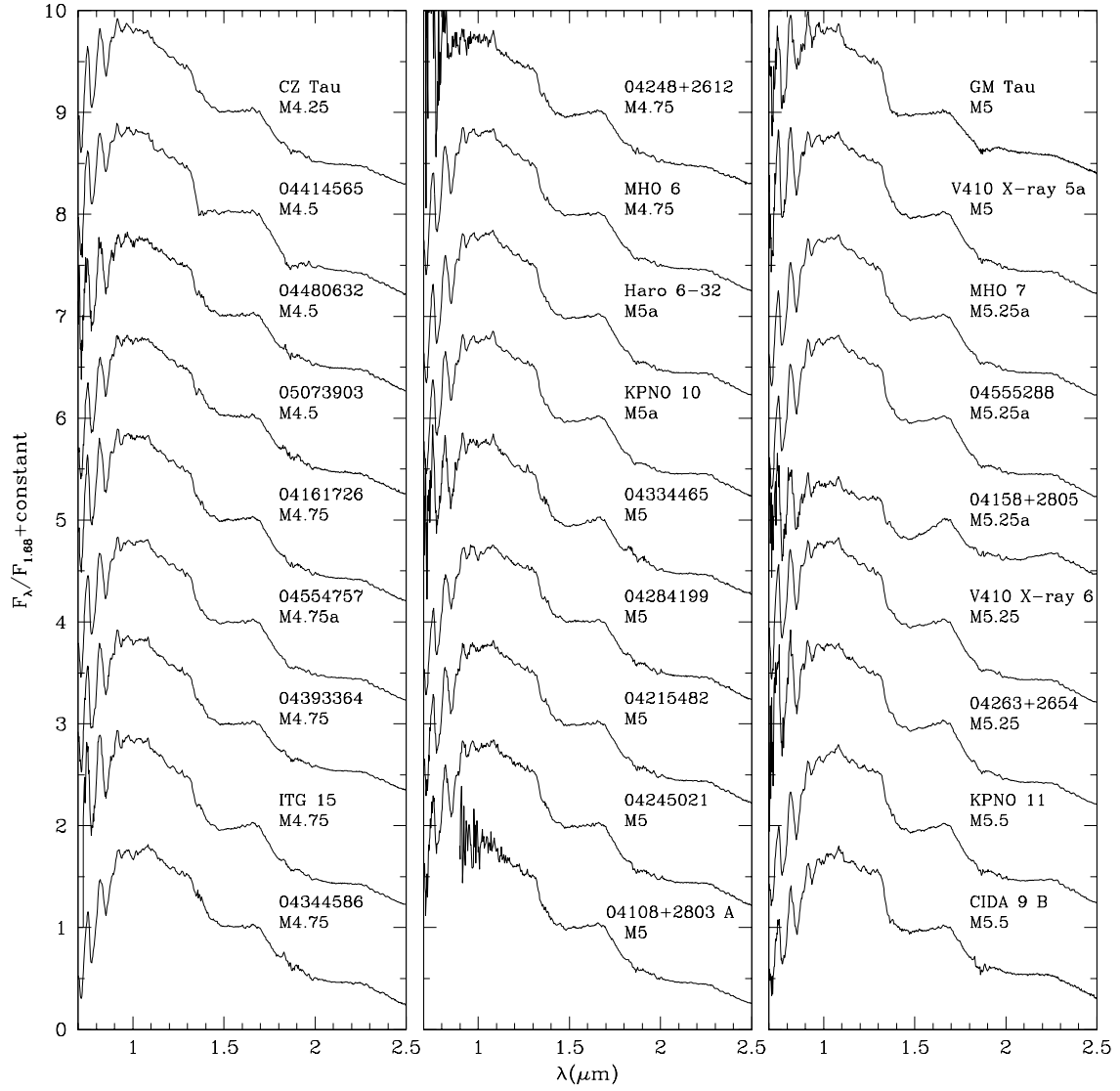


FIG. 9.— More near-IR spectra of members of Taurus (see Figure 5). The data used to create this figure are available.

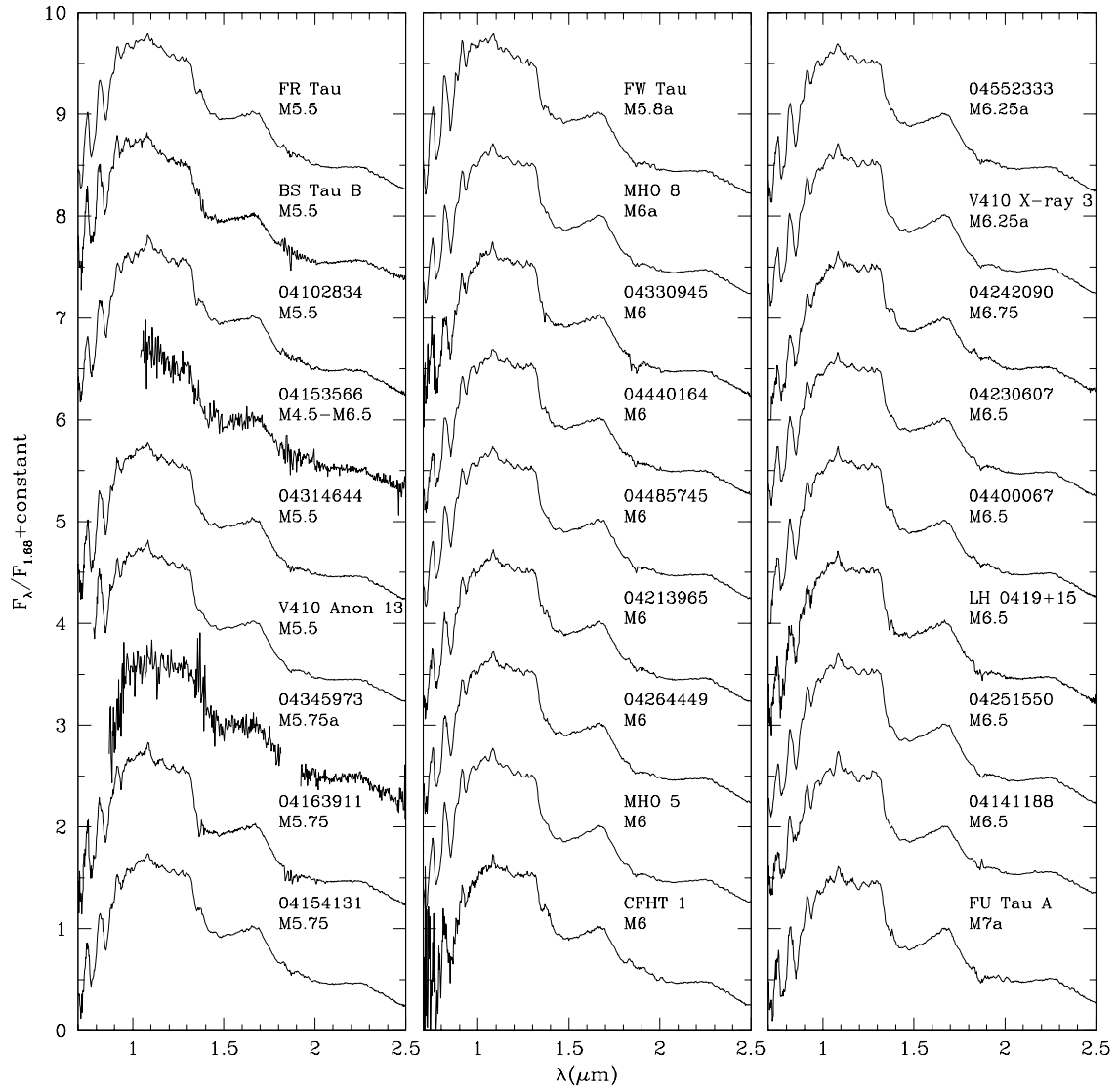


FIG. 10.— More near-IR spectra of members of Taurus (see Figure 5). The data used to create this figure are available.

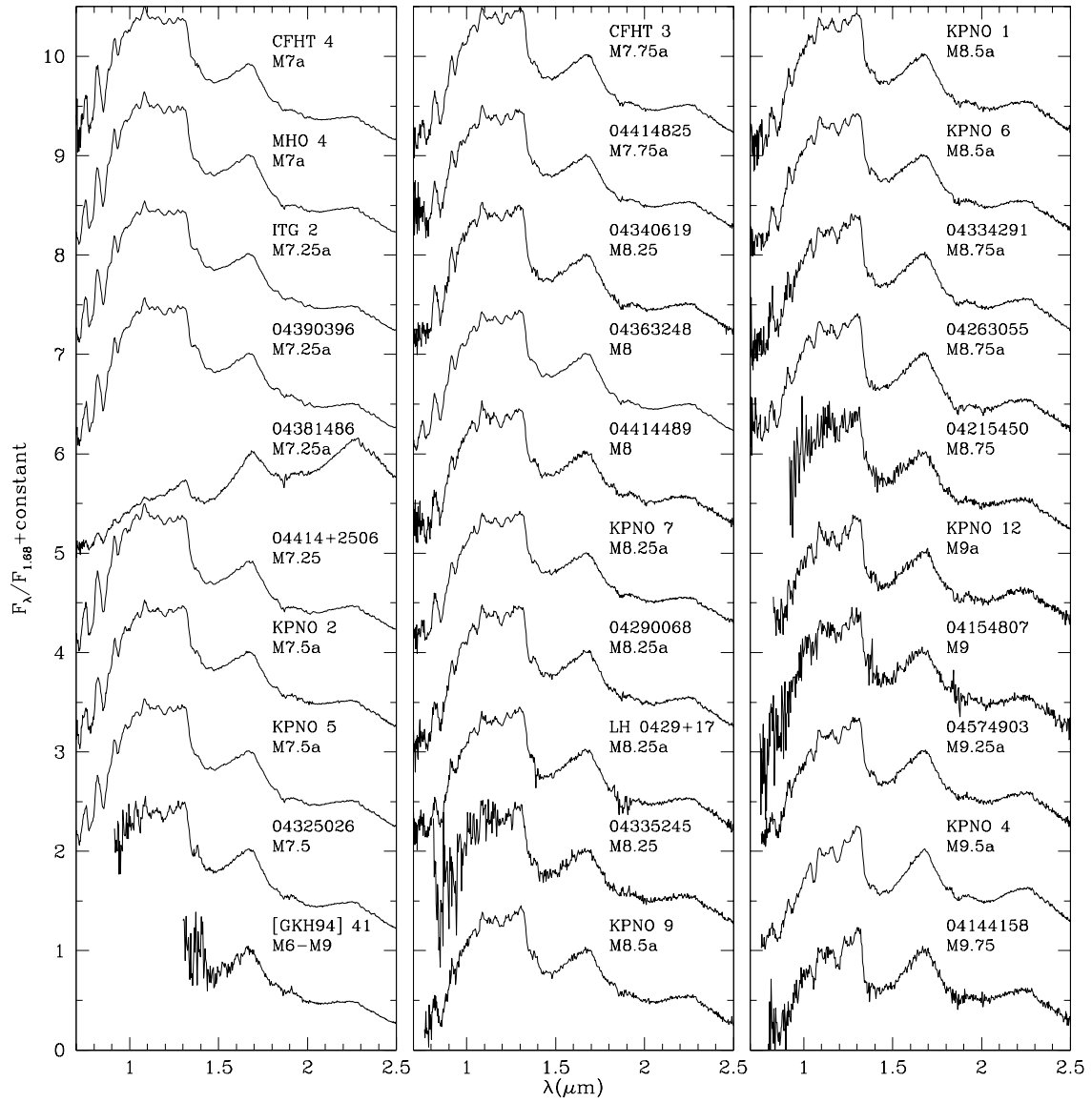


FIG. 11.— More near-IR spectra of members of Taurus (see Figure 5). The spectrum of 2MASS J04381486+2611399 has not been dereddened because it is detected primarily in scattered light (Luhman et al. 2007). The data used to create this figure are available.

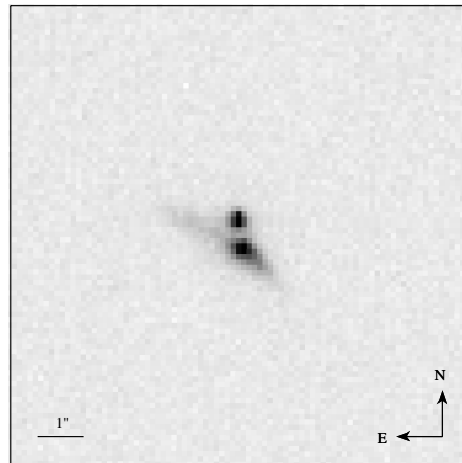


FIG. 12.— NIRC2 K' -band image of the components of 2MASS 04153452+2913469. The size of the field is $10'' \times 10''$.

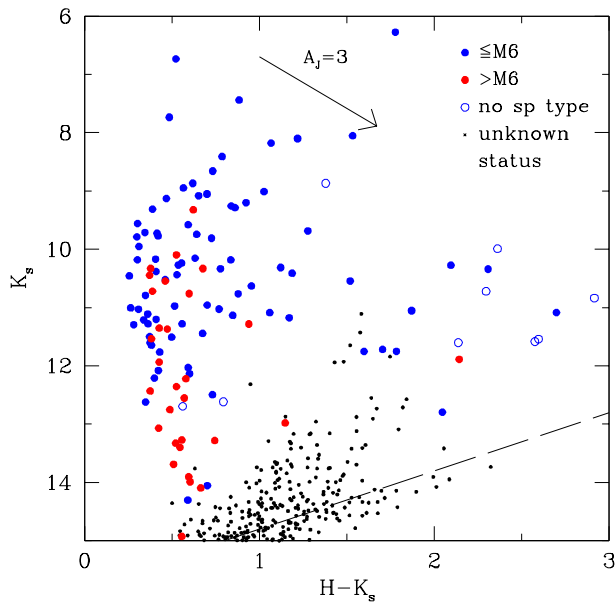


FIG. 13.— CMD from 2MASS for the known members of Taurus (large filled circles) and other sources with unconstrained membership (small points) that are within the SDSS field from Finkbeiner et al. (2004) (Figure 1). We have omitted stars that are likely non-members based on CMDs (Figure 2), proper motions, or spectroscopy. The completeness limit of the 2MASS data is indicated (dashed line).

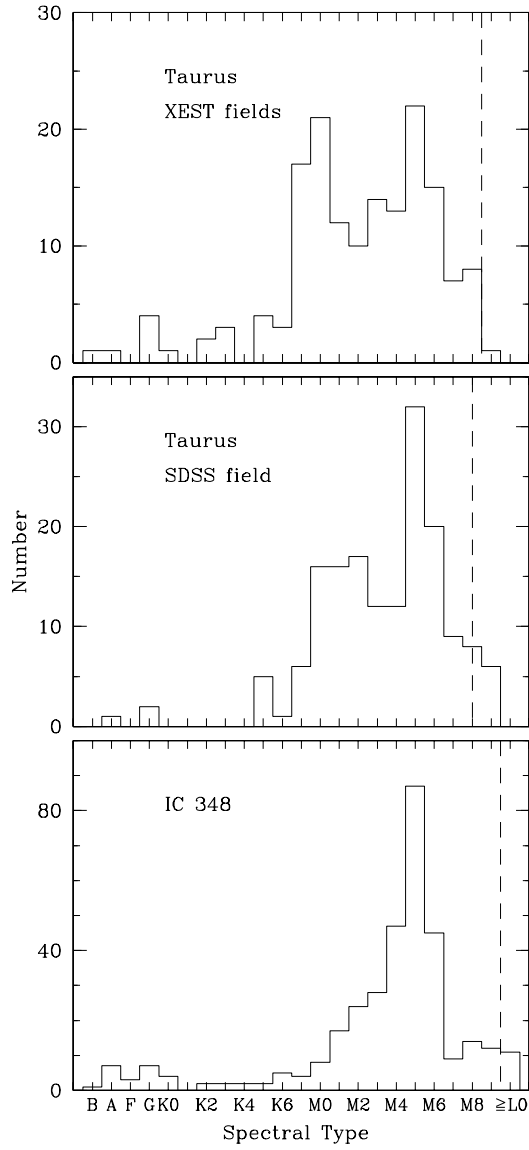


FIG. 14.— Distributions of spectral types for known members of Taurus within the XEST fields (Luhman et al. 2009b), Taurus members with $A_J < 3$ in the SDSS field from Finkbeiner et al. (2004), and members of IC 348 with $A_J < 1.5$ in a field encompassing most of that cluster (Luhman et al. 2016). The completeness limits of these samples of members are indicated (dashed lines).

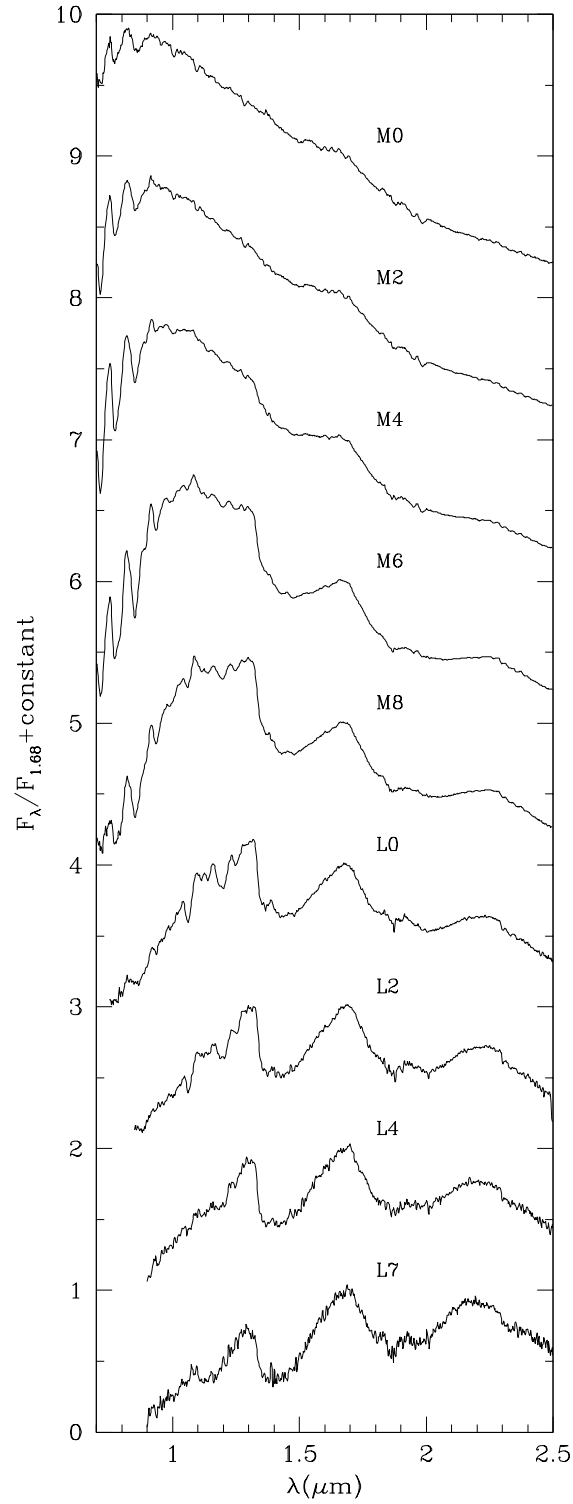


FIG. 15.— Standard spectra for classifying young stars and brown dwarfs, which have been constructed from the SpeX data listed in Table 5. The data used to create this figure are available.

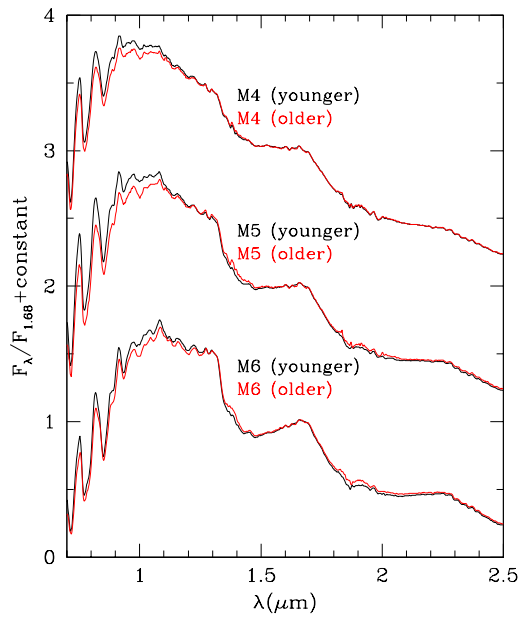


FIG. 16.— Comparisons of the standard spectra constructed from members of younger ($\lesssim 5$ Myr) and older (~ 10 Myr) clusters and associations. On average, the two populations exhibit different 0.7–1.1 μm slopes at mid-M spectral types.

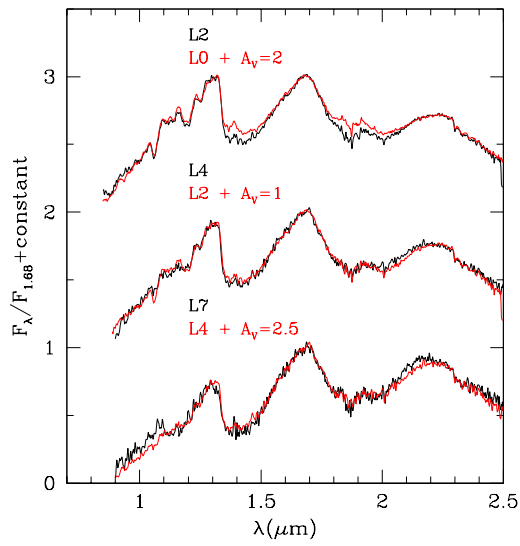


FIG. 17.— Comparisons of standard spectra at L2, L4, and L7 to earlier standards that have been reddened to the same spectral slope. The spectra within each pair are quite similar, which indicates that IR spectral types measured for reddened young L dwarfs (i.e., members of star-forming regions) can have large uncertainties.

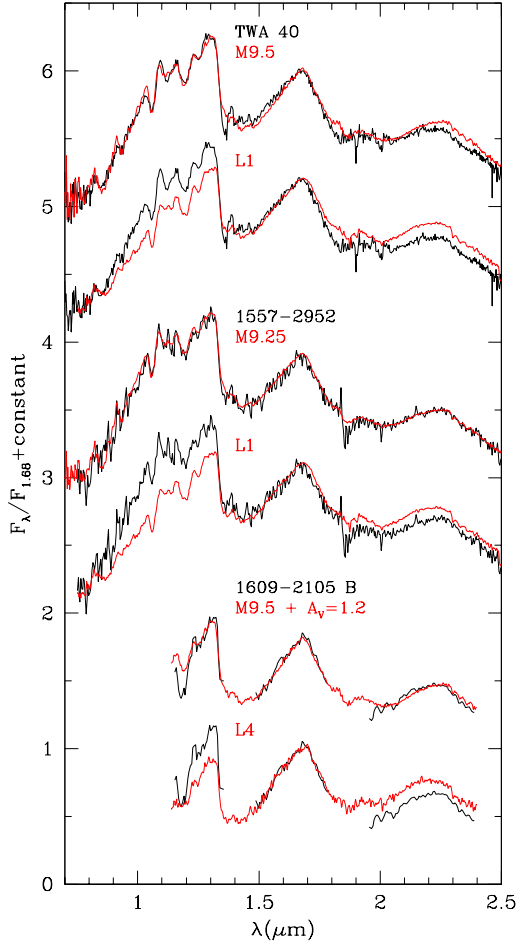


FIG. 18.— Comparisons of spectra of three young late-type objects (Kirkpatrick et al. 2010; Lafrenière et al. 2008, 2010; Gagné et al. 2014) to our best-fitting standard spectra (M9.5, M9.25, M9.5) and our standards for the spectral types from previous studies (L1, L1, L4).